UC San Diego
UC San Diego Previously Published Works

Title
Nonsingular vectorial reformulation of the short-period corrections in Kozai's oblateness solution

Permalink
https://escholarship.org/uc/item/31b6h1vw

Journal
Celestial Mechanics and Dynamical Astronomy, 134(2)

ISSN
0923-2958

Authors

Izzo, Paolo
Dell'Elce, Lamberto
Gurfil, Pini
et al.

Publication Date
2022-04-01

DOI
10.1007/s10569-022-10067-7

Copyright Information

Peer reviewed

Nonsingular vectorial reformulation of the short-period corrections in Kozai's oblateness solution

Paolo Izzo · Lamberto Dell'Elce
Pini Gurfil · Aaron J. Rosengren

Abstract We derive a new analytical solution for the first-order, short-periodic perturbations due to planetary oblateness and systematically compare our results to the classical Brouwer-Lyddane transformation. Our approach is based on the Milankovitch vectorial elements and is free of all the mathematical singularities. Being a non-canonical set, our derivation follows the scheme used by Kozai in his oblateness solution. We adopt the mean longitude as the fast variable and present a compact power-series solution in eccentricity for its short-periodic perturbations that relies on Hansen's coefficients. We also use a numerical averaging algorithm based on the fast-Fourier transform to further validate our new mean-to-osculating and inverse transformations. Only the developed Milankovitch solution was found to accurately handle all regions of the orbital phase space, and it significantly outperforms both Brouwer-Lyddane and the numerical scheme at high eccentricities and inclinations. Improvements should be sought for the low eccentricity and inclination regimes, where the other formulations have an apparent advantage. For a complete first-order theory the long-periodic dynamics, in turn responsible of the critical inclination singularity, should be also included.

1 Introduction

In the brief span of time after the launch of Sputnik, a whole succession of analyses was devoted to the problem poised by the drag-free motion of an artificial satellite about an oblate planet, employing almost every known perturbation method. Although, in a sense, the problem is a classic one that also occurred among the natural satellites, in the applications of artificial satellite motion it was necessary to obtain a more general, detailed, and accurate solution. The most intricate and notable investigations were presented by Brouwer (1959), Garfinkel (1959), and Kozai (1959) in the celebrated 1959 issue of the Astronomical Journal. These authors treat the first- and second-order secular perturbations, as well as the first-order short-periodic (related to the satellite's mean motion) and long-periodic (related to the evolution of the argument of the perigee) perturbations of the orbital elements, where order here refers to the oblateness parameter.

Astronomical experience amply bears out the notion of separation of perturbing effects into periodic and secular variations and the distinction between fast and slow time variables concerning the motion of

---

Paolo Izzo
Technion–Israel Institute of Technology, 32000 Haifa, Israel
Sapienza University of Rome, 00138 Rome, Italy
E-mail: p.izzo@uniroma1.it

Lamberto Dell'Elce
Université Côte Azur and Inria Sophia Antipolis Méditerranée, 06902 Valbonne, France

Pini Gurfil
Technion–Israel Institute of Technology, 32000 Haifa, Israel

Aaron J. Rosengren
Department of Mechanical and Aerospace Engineering, UC San Diego, La Jolla, CA 92093, USA

satellites (Lara 2019). The device of canonical transformations employed by Brouwer (1959) and Garfinkel (1959) permits a deeper understanding of the difference between periodic and secular perturbations, and provides a systematic procedure for the inclusion of higher-order terms (Kozai 1962b). On the other hand, the technique used by Kozai (1959), known formally as the method of analytic continuation (Scheeres 2012), while applicable to any set of orbital elements, canonical or otherwise, can be cumbersome beyond the first order. The Poincaré-von Zeipel method of canonical transformations, though still in use (Nie et al 2019), was significantly generalized by Hori (1966) and Deprit (1969) based on Lie series; the latter becoming the *sine qua non* of modern perturbation theory in celestial mechanics (Deprit and Rom 1970; Kaufman 1981).

Kozai's gravity solution to the artificial satellite problem became the basis for the simplified general perturbations theory, SGP, that would be supplanted by SGP4, an analytical solution for satellite short-term prediction using the two-line element sets that instead has its roots in Brouwer's gravitational theory (Hoots et al 2004). Brouwer (1959) developed his original solution in Delaunay variables, the canonically-conjugate counterpart of the Keplerian orbital elements used by Kozai (1959), which, like the classical ones themselves, are singular for circular and equatorial orbits. The mathematical singularities associated with zero eccentricity and vanishing line of nodes that plague these solutions can be removed by reformulating them in nonsingular variables, such as those of Poincaré (Lyddane 1963; Breakwell and Vagners 1970), Hill (Izsak 1963; Aksnes 1972), or the equinoctial set (Gim and Alfriend 2003; Alfriend et al 2009; Le Fèvre et al 2014),[1] or Euler-parameters-based elements (Alfriend et al 2009). A simplified form of the Lyddane-modified Brouwer theory, optimized in SGP4 for the rapid propagation of satellite ephemerides of the space object catalog (SOC) (Hoots 1981), is the basis for many tracking and prediction operations. Moreover, SGP4, or its deep space equivalent, SDP4, must be used to convert the mean, orbit-averaged, TLEs of the SOC into an osculating set of elements for use in special perturbation theory to obtain more accurate predictions (Levit and Marshall 2011).

The principal observable features due to Earth's oblateness are a secular precession of the orbit plane about the polar axis and a steady motion of the major axis in the moving orbit plane. Well-known applications of this particular problem are the two inclined and elliptical orbit systems (12-hr Molniya and 24-hr Tundra), placed at the reputed critical inclination of $\sim63.4°$ so that the apsidal precession freezes on average. The critical inclination is an intrinsic singularity in the artificial satellite theories of our forebears (Coffey et al 1986), and hitherto remains a fundamental issue in all modern reformulations of the main problem (Breakwell and Vagners 1970; Aksnes 1972; Lara 2015b,a). The orbit-averaging technique fundamentally involves removing all terms that depend on the fast-varying mean anomaly, thus retaining the (secular and long-period) mean-element motion. As noted by Kozai (1959), the long-periodic perturbations of the first order come from the terms of the second order, and the singularity associated with the critical inclination only arises when such long-period effects are retained. Nevertheless, the distinction between secular and mean elements has often been muddled in the literature, and tabulated mean-to-osculating transformations (Gim and Alfriend 2003; Schaub and Junkins 2018) apply Brouwer's full periodic corrections. This approach will inevitably lead to significant errors near the critical inclination, but can be properly amended by neglecting the long-periodic terms (Breakwell and Vagners 1970).

An important application of the mean-to-osculating transformation is in the computation of the nominal osculating orbits from the frozen-orbit conditions determined in mean-elements space (Gurfil and Lara 2013). Frozen orbits correspond to equilibria for the averaged equations of motion, and, in the oblateness model, occur when secular effects due to even zonal harmonics are canceled by the long-period perturbations of the odd harmonics. While modern formulations compute frozen orbits directly from the non-averaged equations, based on the underlying quasi-periodic structure of librations around these mean equilibria, explicit analytical solutions form the starting point for the numerical optimization process. Recovering the short-periodic effects needed for this initialization can be troublesome at the critical inclination, whose precise frozen-orbit location is very sensitive to model truncation (Lara 2018).

Here, we present a new formulation of the mean-to-osculating and inverse conversions for first-order oblateness perturbations based on the Milankovitch elements (Rosengren and Scheeres 2013, 2014). We use the direct method of Kozai (1959), as further elucidated by Scheeres (2012), and present an explicit analytical short-period correction in vector form that is valid for all elliptical orbits. We adopt the mean longitude as the fast variable and present a compact power-series solution in eccentricity for its short-periodic perturbations that can be truncated to achieve the necessary accuracy. We establish a truth model using a numerical averaging approach based on the fast-Fourier transform (Uphoff 1973; Ely 2015), and make detailed comparisons between our vectorial solution and the classical Brouwer-Lyddane (BL) theory.

---

[1] The open-source and extensively validated tool, Semi-analytic Tool for End of Life Analysis (STELA), developed by CNES, is also based on the equinoctial parameters (Le Fèvre et al 2014).

For the latter, we adapt the more streamlined formulas presented in Schaub and Junkins (2018) and Gim and Alfriend (2003).

2 Problem formulation

2.1 Analytical averaging

The basic idea in orbit-averaging methods is to obtain approximate equations for the system evolution that contain only slowly changing variables by exploiting the presence of a small dimensionless parameter ϵ that characterizes the size of the perturbation. The tacit assumption is that the perturbing forces are sufficiently weak so that these approximate mean equations of motion can be used to describe the secular and long-period orbital evolution. The perturbation equations in celestial mechanics, relating the time variation of the orbit parameters to the perturbing accelerations, in Gauss or Lagrange form, are nonlinear, nonautonomous, first-order differential equations: (Alfriend et al 2009; Scheeres 2012)

$$\dot{\boldsymbol{x}} = \epsilon \boldsymbol{g}(\boldsymbol{x}, t), \tag{1}$$

in which $\boldsymbol{g}(\boldsymbol{x}, t)$ is assumed to be T-periodic in time t. Equation (1) is trivially solved when $\epsilon = 0$, yielding the integrals (Keplerian elements) in the unperturbed problem. The method of averaging consists of replacing Equation (1) by the averaged autonomous system (Sanders et al 2007)

$$\dot{\overline{\boldsymbol{x}}} = \epsilon \overline{\boldsymbol{g}}(\overline{\boldsymbol{x}}), \qquad \overline{\boldsymbol{g}}(\overline{\boldsymbol{x}}) = \frac{1}{T} \int_0^T \boldsymbol{g}(\overline{\boldsymbol{x}}, t) \, \mathrm{d}t, \tag{2}$$

where the average is performed over time, and it is understood that $\overline{\boldsymbol{x}}$ in the integrand is to be regarded as a constant during the averaging process. The basis for this approximation is the averaging principle, which states that in the general, non-resonant case, the short-period terms removed by averaging cause only small oscillations that are superimposed on the long-term solution described by the averaged system.

Comparison between numerical integrations and the mean solution will in general show a divergence between the two as a result of an inconsistent choice of initial conditions, as depicted in Fig. 1. This offset can be understood by decomposing the osculating elements into mean and short-period components (Kozai 1959; Scheeres 2012):

$$\boldsymbol{x}(t) = \overline{\boldsymbol{x}}(t) + \boldsymbol{x}^{sp}(t). \tag{3}$$

Differentiating, we can obtain an approximate equation governing the short-period dynamics:

$$\dot{\boldsymbol{x}}^{sp}(t) = \dot{\boldsymbol{x}} - \dot{\overline{\boldsymbol{x}}} \cong \boldsymbol{g}(\overline{\boldsymbol{x}}, t) - \overline{\boldsymbol{g}}(\overline{\boldsymbol{x}}), \tag{4}$$

in which the mean state $\overline{\boldsymbol{x}}$ has replaced the corresponding osculating elements $\boldsymbol{x}$ in the dynamical equations and where the small parameter ϵ has been omitted without lack of generality. From Eqs. (3) and (4), the short-periodic perturbations can be obtained as (Kozai 1959)

$$\boldsymbol{x}^{sp}(t) = \mathrm{d}\boldsymbol{x}^{sp}(t) - \overline{\mathrm{d}\boldsymbol{x}}^{sp} = \int [\boldsymbol{g}(\overline{\boldsymbol{x}}, t) - \overline{\boldsymbol{g}}(\overline{\boldsymbol{x}})] \, \mathrm{d}t - \frac{1}{T} \int_0^T \int [\boldsymbol{g}(\overline{\boldsymbol{x}}, t) - \overline{\boldsymbol{g}}(\overline{\boldsymbol{x}})] \, \mathrm{d}t^2. \tag{5}$$

Accordingly, it can be seen that $\overline{\boldsymbol{x}}^{sp} = \boldsymbol{0}$, which is also the implicit assumption in the averaging process.

The interpretation of this result is that given an initial condition for a state $\boldsymbol{x}_0 = \boldsymbol{x}(t_0)$, the mean equations have to be initialized at a value provided by Eqs. (3) and (5) as

$$\overline{\boldsymbol{x}}_0 = \boldsymbol{x}_0 - \boldsymbol{x}^{sp}(t_0), \tag{6}$$

to have the averaged dynamics track the true evolution more closely.

The removal of time, or analogously of the mean anomaly, requires computing the quadrature of functions depending implicitly on this variable through the true anomaly. The time averaging is performed over a periodic motion having a period much shorter than the time that characterizes the evolution of the dynamical system; this periodicity necessarily implies that averaging is taken for elliptical orbits. Given a quantity $\boldsymbol{g}(\boldsymbol{x}, M)$ representing the right-hand side of the equations of motion, defined as a function of the
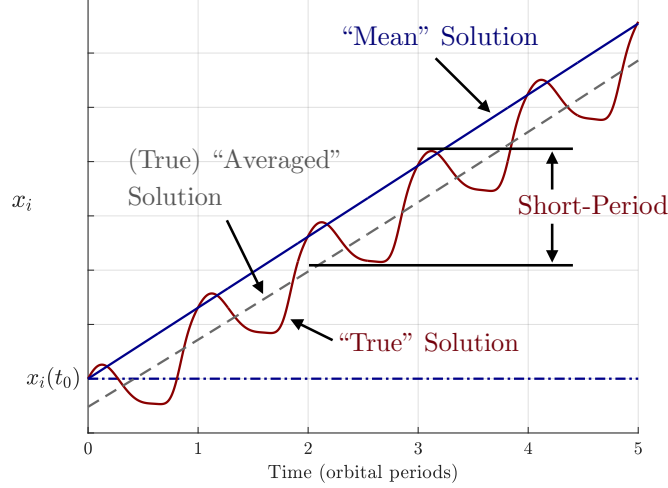
Fig. 1 Schematic showing a comparison between the numerical and mean solutions for an arbitrary orbital element, when starting from the same initial condition. The mean solution changes approximately linearly over one orbit and is referred to as the averaged variation. The short-period oscillations are the fluctuations that happen per orbit in the real motion.

dimensionless time variable M (the mean anomaly) in addition to the other orbital elements given by $\boldsymbol{x}$, the average, Eq. (2), can be redefined as

$$\overline{\boldsymbol{g}}(\overline{\boldsymbol{x}}) = \frac{1}{2\pi} \int_0^{2\pi} \boldsymbol{g}(\overline{\boldsymbol{x}}, M) \, \mathrm{d}M, \tag{7}$$

where the orbital elements $\overline{\boldsymbol{x}}$ are held constant in the integration. Although the average is defined with respect to mean anomaly, it is often more easily calculated by means of the true or eccentric anomaly, f and E, respectively, using the differential relationships

$$\mathrm{d}M = \frac{r}{a}\mathrm{d}E = \frac{r^2}{ab}\mathrm{d}f, \tag{8}$$

in which a and $b = a\sqrt{1 - e^2}$ are the semi-major and semi-minor axes, respectively, and e is the eccentricity; yielding the equivalent forms for averaging:

$$\overline{\boldsymbol{g}}(\overline{\boldsymbol{x}}) = \frac{1}{2\pi} \int_0^{2\pi} \boldsymbol{g}(\overline{\boldsymbol{x}}, M) \, \mathrm{d}M = \frac{1}{2\pi a} \int_0^{2\pi} \boldsymbol{g}(\overline{\boldsymbol{x}}, E) \, r \, \mathrm{d}E = \frac{1}{2\pi ab} \int_0^{2\pi} \boldsymbol{g}(\overline{\boldsymbol{x}}, f) \, r^2 \, \mathrm{d}f. \tag{9}$$

Note that r can be expressed in terms of f and E as

$$r = \begin{cases} \dfrac{a(1 - e^2)}{1 + e \cos f} = \dfrac{H^2/\mu}{1 + e \cos f}, \\[2ex] a(1 - e \cos E). \end{cases} \tag{10}$$

Here, H is the specific angular momentum and μ is the gravitational parameter.

The Milankovitch elements consist of the two fundamental vectorial integrals of motion, namely, the eccentricity vector $\boldsymbol{e}$ and angular momentum vector $\boldsymbol{H}$. These vectors can be parameterized in terms of the Keplerian elements relative to an inertial frame:

$$\boldsymbol{H} = H\hat{\boldsymbol{h}} = H(\sin i \sin \Omega \hat{\boldsymbol{x}} - \sin i \cos \Omega \hat{\boldsymbol{y}} + \cos i \hat{\boldsymbol{z}}), \tag{11}$$

$$\begin{aligned} \boldsymbol{e} = e\hat{\boldsymbol{e}} \ = e\big[&(\cos \omega \cos \Omega - \cos i \sin \omega \sin \Omega)\hat{\boldsymbol{x}} \\ &+ (\cos \omega \sin \Omega + \cos i \sin \omega \cos \Omega)\hat{\boldsymbol{y}} \\ &+ \sin i \sin \omega \hat{\boldsymbol{z}}\big], \end{aligned} \tag{12}$$

where i is the inclination, Ω is the right ascension of the ascending node, and ω is the argument of periapsis. Because of the orthogonality constraint (i.e., $\boldsymbol{H} \cdot \boldsymbol{e} = 0$) we need a sixth scalar element to fully define an orbit (Roy and Moran 1973). Adopting the mean longitude $l = \omega + \Omega + M$, the non-averaged equations of motion

4

for an arbitrary disturbing acceleration $\boldsymbol{a}_d$ can be stated in 'dyadic' form[2] as (Battin 1999; Rosengren and Scheeres 2014):

$$\dot{\boldsymbol{e}} = \frac{1}{\mu}\left(\widetilde{\boldsymbol{v}}\cdot\widetilde{\boldsymbol{r}} - \widetilde{\boldsymbol{H}}\right)\cdot\boldsymbol{a}_d = \boldsymbol{g}_e(\boldsymbol{x},t), \tag{13a}$$

$$\dot{\boldsymbol{H}} = \widetilde{\boldsymbol{r}}\cdot\boldsymbol{a}_d = \boldsymbol{g}_H(\boldsymbol{x},t), \tag{13b}$$

$$\dot{l} = n + \left(-\frac{e}{\mu(1+\sqrt{1-e^2})}\left[H(\hat{\boldsymbol{e}}\cdot\hat{\boldsymbol{r}})\hat{\boldsymbol{r}} + (r+p)(\hat{\boldsymbol{e}}\cdot\boldsymbol{v})\hat{\boldsymbol{\theta}}\right] - \frac{2}{na^2}\boldsymbol{r} + \frac{\boldsymbol{r}\cdot\hat{\boldsymbol{z}}}{H(H+\boldsymbol{H}\cdot\hat{\boldsymbol{z}})}\boldsymbol{H}\right)\cdot\boldsymbol{a}_d,$$
$$= n + g_l(\boldsymbol{x},t), \tag{13c}$$

where $n^2 = \mu/a^3$, $p = H^2/\mu$, and $\hat{\boldsymbol{\theta}} = \widetilde{\hat{\boldsymbol{h}}}\cdot\hat{\boldsymbol{r}}$. Note that Eq. (13c) consists of terms that collect the contributions due to the three components in the radial, transverse, and normal directions of the disturbing acceleration, and is valid for elliptical orbits in which $e < 1$.

The position and velocity vectors, $\boldsymbol{r}$ and $\boldsymbol{v}$, may be expressed as

$$\boldsymbol{r} = r\left(\cos f\hat{\boldsymbol{e}} + \sin f\hat{\boldsymbol{e}}_\perp\right), \tag{14}$$

$$\boldsymbol{v} = \frac{\mu}{H}\left[-\sin f\hat{\boldsymbol{e}} + (e+\cos f)\hat{\boldsymbol{e}}_\perp\right], \tag{15}$$

where $\hat{\boldsymbol{e}} = \boldsymbol{e}/e$, $\hat{\boldsymbol{e}}_\perp = \widetilde{\hat{\boldsymbol{h}}}\cdot\hat{\boldsymbol{e}}$, and $\hat{\boldsymbol{h}} = \boldsymbol{H}/H$.

The Gauss equations have time-varying terms multiplying the accelerations involving the true anomaly, and thus they must each be averaged separately. The mean evolution of these elements can be computed as

$$\dot{\overline{\boldsymbol{e}}} = \frac{1}{2\pi}\int_0^{2\pi}\dot{\boldsymbol{e}}\,\mathrm{d}M = \overline{\boldsymbol{g}}_e(\overline{\boldsymbol{x}}), \tag{16a}$$

$$\dot{\overline{\boldsymbol{H}}} = \frac{1}{2\pi}\int_0^{2\pi}\dot{\boldsymbol{H}}\,\mathrm{d}M = \overline{\boldsymbol{g}}_H(\overline{\boldsymbol{x}}), \tag{16b}$$

$$\dot{\overline{l}} = \frac{1}{2\pi}\int_0^{2\pi}\dot{l}\,\mathrm{d}M = \overline{n} + \overline{g}_l(\overline{\boldsymbol{x}}). \tag{16c}$$

The approximate short-period equations of motion for each element can then be formulated by subtracting Eq. (16) from Eq. (13), while holding all orbital elements but f constant. Kozai (1959), in his solution employing the classical elements a, e, i, Ω, ω, and M, obtained the non-averaged, mean, and short-period equations of motion using the Lagrange planetary equations. We note that a more general procedure has been outlined herein.

Particularly, for $\boldsymbol{e}$ and $\boldsymbol{H}$, following Eq. (5), we have

$$\mathrm{d}\boldsymbol{e}^{sp}(t) = \int\left[\boldsymbol{g}_e(\overline{\boldsymbol{x}},t) - \overline{\boldsymbol{g}}_e(\overline{\boldsymbol{x}})\right]\mathrm{d}t, \tag{17a}$$

$$\mathrm{d}\boldsymbol{H}^{sp}(t) = \int\left[\boldsymbol{g}_H(\overline{\boldsymbol{x}},t) - \overline{\boldsymbol{g}}_H(\overline{\boldsymbol{x}})\right]\mathrm{d}t, \tag{17b}$$

so that

$$\boldsymbol{e}^{sp}(t) = \mathrm{d}\boldsymbol{e}^{sp}(t) - \overline{\mathrm{d}\boldsymbol{e}}^{sp}, \tag{18a}$$

$$\boldsymbol{H}^{sp}(t) = \mathrm{d}\boldsymbol{H}^{sp}(t) - \overline{\mathrm{d}\boldsymbol{H}}^{sp}. \tag{18b}$$

Special care, however, must be taken in the case of the mean longitude due to the presence of the mean motion appearing without any factor in Eq. (13c) (Kozai 1959). Expanding the osculating n into a first-order Taylor series about the mean elements, and following Eq. (4), we can write the approximate equation governing the short-period dynamics as

$$l^{sp}(t) = \dot{l} - \dot{\overline{l}} \cong g_l(\overline{\boldsymbol{x}},t) - \overline{g}_l(\overline{\boldsymbol{x}}) + \nabla_{\boldsymbol{e}}n(\overline{\boldsymbol{x}})\cdot\boldsymbol{e}^{sp}(t) + \nabla_{\boldsymbol{H}}n(\overline{\boldsymbol{x}})\cdot\boldsymbol{H}^{sp}(t), \tag{19}$$

---

[2] An expression $\boldsymbol{ab}$, formed by the juxtaposition of two vectors in R^3 constitutes what is called a dyad. For notational convenience, we denote the cross-product dyadic as $\widetilde{\boldsymbol{a}}$ so that the *tilde* operator turns a vector into a skew-symmetric dyadic, allowing to write the cross product as a linear vector function. Equivalent expressions of the cross product are: $\boldsymbol{a}\times\boldsymbol{b} = \widetilde{\boldsymbol{a}}\cdot\boldsymbol{b} = \boldsymbol{a}\cdot\widetilde{\boldsymbol{b}} = -\widetilde{\boldsymbol{b}}\cdot\boldsymbol{a} = -\boldsymbol{b}\cdot\widetilde{\boldsymbol{a}}$.

where

$$\nabla_{\boldsymbol{e}}n(\overline{\boldsymbol{x}}) = \left.\frac{\partial n}{\partial \boldsymbol{e}}\right|_{\boldsymbol{x}=\overline{\boldsymbol{x}}} = -\frac{3\mu^2}{\overline{H}^3}\sqrt{1-\overline{e}^2}\,\overline{\boldsymbol{e}}, \tag{20}$$

$$\nabla_{\boldsymbol{H}}n(\overline{\boldsymbol{x}}) = \left.\frac{\partial n}{\partial \boldsymbol{H}}\right|_{\boldsymbol{x}=\overline{\boldsymbol{x}}} = -\frac{3\mu^2}{\overline{H}^5}(1-\overline{e}^2)^{3/2}\,\overline{\boldsymbol{H}}. \tag{21}$$

Accordingly,

$$\mathrm{d}l^{sp}(t) = \int\left[g_l(\overline{\boldsymbol{x}},t) - \overline{g}_l(\overline{\boldsymbol{x}})\right]\mathrm{d}t + \nabla_{\boldsymbol{e}}n(\overline{\boldsymbol{x}})\cdot\int\boldsymbol{e}^{sp}(t)\,\mathrm{d}t + \nabla_{\boldsymbol{H}}n(\overline{\boldsymbol{x}})\cdot\int\boldsymbol{H}^{sp}(t)\,\mathrm{d}t, \tag{22}$$

and

$$\begin{aligned}\overline{\mathrm{d}l}^{sp} = \frac{1}{T}\int_0^T\int\left[g_l(\overline{\boldsymbol{x}},f) - \overline{g}_l(\overline{\boldsymbol{x}})\right]\mathrm{d}t^2\\ + \nabla_{\boldsymbol{e}}n(\overline{\boldsymbol{x}})\cdot\frac{1}{T}\int_0^T\int\boldsymbol{e}^{sp}(t)\,\mathrm{d}t^2 + \nabla_{\boldsymbol{H}}n(\overline{\boldsymbol{x}})\cdot\frac{1}{T}\int_0^T\int\boldsymbol{H}^{sp}(t)\,\mathrm{d}t^2.\end{aligned} \tag{23}$$

As a result, the short-periodic perturbations of l is given by

$$l^{sp}(t) = \mathrm{d}l^{sp}(t) - \overline{\mathrm{d}l}^{sp}. \tag{24}$$

2.2 Numerical averaging

The conversion between mean and osculating elements can be obtained numerically, as previously shown by Walter (1967), Uphoff (1973), and Ely (2015). Here, we will exploit a numerical implementation of the near-identity transformation in Eq. (3) between averaged and osculating Milankovitch elements to validate our subsequent analytical developments.

The mapping is obtained by numerically solving

$$\begin{aligned}\frac{\partial\,\boldsymbol{x}^{sp}}{\partial\,t} &= \epsilon\left[\boldsymbol{g}\left(\overline{\boldsymbol{x}},t\right) - \overline{\boldsymbol{g}}\left(\overline{\boldsymbol{x}}\right)\right],\\ \int_0^T\boldsymbol{x}^{sp}(\overline{\boldsymbol{x}},t)\,\mathrm{d}t &= \boldsymbol{0}.\end{aligned} \tag{25}$$

The boundary condition in Eq. (25) guarantees that the oscillations of $\boldsymbol{x}^{sp}(t)$ are unbiased with respect to $\overline{\boldsymbol{x}}$. The formal solution is then (Sanders et al 2007)

$$\boldsymbol{x}^{sp}\left(\overline{\boldsymbol{x}},t\right) = -\epsilon\frac{i}{n}\sum_{k=1}^{\infty}\frac{c_k\left(\overline{\boldsymbol{x}}\right)}{k}e^{iknt}, \tag{26}$$

where $c_k\left(\overline{\boldsymbol{x}}\right)$ are the Fourier coefficients of $\boldsymbol{g}\left(\overline{\boldsymbol{x}},t\right)$, and i is the imaginary unit.

In this study, we numerically approximate Eq. (26) by truncating the series and by using the fast-Fourier transform (FFT) algorithm as discussed in Ely (2015), under the assumption that $\boldsymbol{g}$ is analytic on the continuation of nt in a non-vanishing complex strip. This assumption guarantees that the Fourier coefficients exhibit exponential decrease as a function of k. For the mean orbit longitude, we incorporate the additional terms in Eq. (19), resulting from the Taylor series of n, into Eq. (25), before performing the numerical quadrature.

6

3 Analytical short-period correction for oblateness perturbations

The quadrupolar (i.e., J_2-truncated) disturbing function arising from an oblate planet can be stated in a general vector expression as (Scheeres 2012)

$$\mathcal{R} = \frac{\mu J_2 R^2}{2r^3}\left[1 - 3(\hat{\boldsymbol{r}}\cdot\hat{\boldsymbol{p}})^2\right], \tag{27}$$

where J_2 is the second zonal harmonic coefficient, R is the mean equatorial radius of the planet, and $\hat{\boldsymbol{r}} = \boldsymbol{r}/r$ from Eq. (14). Note that the Earth's spin axis $\hat{\boldsymbol{p}}$ is assumed to be fixed in inertial space, and, as such, is aligned with $\hat{\boldsymbol{z}}$.

The perturbing acceleration is then given by $\partial\mathcal{R}/\partial\boldsymbol{r}$ as

$$\boldsymbol{a} = -\frac{3\mu J_2 R^2}{2r^5}\left\{\left[1 - 5(\hat{\boldsymbol{r}}\cdot\hat{\boldsymbol{p}})^2\right]\boldsymbol{r} + 2(\boldsymbol{r}\cdot\hat{\boldsymbol{p}})\hat{\boldsymbol{p}}\right\}. \tag{28}$$

Accordingly, following Eq. (13), the perturbation equations can be stated as

$$\dot{\boldsymbol{e}} = \frac{3J_2 R^2}{2r^5}\left\{\left[1 - 5(\hat{\boldsymbol{r}}\cdot\hat{\boldsymbol{p}})^2\right]\widetilde{\boldsymbol{H}}\cdot\boldsymbol{r} - 2(\boldsymbol{r}\cdot\hat{\boldsymbol{p}})(\widetilde{\boldsymbol{v}}\cdot\widetilde{\boldsymbol{r}} - \widetilde{\boldsymbol{H}})\cdot\hat{\boldsymbol{p}}\right\}, \tag{29a}$$

$$\dot{\boldsymbol{H}} = -\frac{3\mu J_2 R^2}{r^5}(\boldsymbol{r}\cdot\hat{\boldsymbol{p}})\widetilde{\boldsymbol{r}}\cdot\hat{\boldsymbol{p}}, \tag{29b}$$

$$\dot{l} = n + \frac{3\mu J_2 R^2}{2r^5}\left\{\frac{1}{\mu(1+\sqrt{1-e^2})}\left[H(\boldsymbol{e}\cdot\boldsymbol{r})(1 - 3(\hat{\boldsymbol{r}}\cdot\hat{\boldsymbol{p}})^2) + 2(r+p)(\boldsymbol{e}\cdot\boldsymbol{v})(\boldsymbol{r}\cdot\hat{\boldsymbol{p}})(\hat{\boldsymbol{\theta}}\cdot\hat{\boldsymbol{p}})\right] \right.$$
$$\left. + \frac{2r^2}{na^2}(1 - 3(\hat{\boldsymbol{r}}\cdot\hat{\boldsymbol{p}})^2) - \frac{2(\boldsymbol{r}\cdot\hat{\boldsymbol{p}})^2(\boldsymbol{H}\cdot\hat{\boldsymbol{p}})}{H(H + \boldsymbol{H}\cdot\hat{\boldsymbol{p}})}\right\}. \tag{29c}$$

The averaged equations of motion for the eccentricity and angular momentum vectors are given by Ward (1962) and Rosengren and Scheeres (2013). Averaging Eq. (29c) directly requires computing the quadrature of various dyadics and higher rank tensors of the dynamical variables, the details of which we omit. The mean equations can be stated as

$$\dot{\bar{\boldsymbol{e}}} = -\frac{3nJ_2 R^2}{4p^2}\left\{\left[1 - 5(\hat{\boldsymbol{h}}\cdot\hat{\boldsymbol{p}})^2\right]\widetilde{\hat{\boldsymbol{h}}} + 2(\hat{\boldsymbol{h}}\cdot\hat{\boldsymbol{p}})\widetilde{\hat{\boldsymbol{p}}}\right\}\cdot\boldsymbol{e}, \tag{30a}$$

$$\dot{\bar{\boldsymbol{H}}} = \frac{3HnJ_2 R^2}{2p^2}(\hat{\boldsymbol{h}}\cdot\hat{\boldsymbol{p}})\widetilde{\hat{\boldsymbol{h}}}\cdot\hat{\boldsymbol{p}}, \tag{30b}$$

$$\dot{\bar{l}} = n + \frac{3nJ_2 R^2}{4p^2}\left\{\sqrt{1-e^2}\left[3(\hat{\boldsymbol{h}}\cdot\hat{\boldsymbol{p}})^2 - 1\right] + 5(\hat{\boldsymbol{h}}\cdot\hat{\boldsymbol{p}})^2 - 2(\hat{\boldsymbol{h}}\cdot\hat{\boldsymbol{p}}) - 1\right\}, \tag{30c}$$

where the bar operator is omitted from the elements because there is no ambiguity in what follows; i.e., all variables are averaged variables. Note that Eq. (30c) can be seen as the sum of the classical secular precession rates arising from planetary oblateness, $\dot{\bar{l}} = \dot{\bar{M}} + \dot{\bar{\omega}} + \dot{\bar{\Omega}}$, where

$$\dot{\bar{M}} = n + \frac{3nJ_2 R^2}{4p^2}\sqrt{1-e^2}\left(3\cos^2 i - 1\right),\ \dot{\bar{\omega}} = \frac{3nJ_2 R^2}{4p^2}\left(5\cos^2 i - 1\right),\ \dot{\bar{\Omega}} = -\frac{3nJ_2 R^2}{2p^2}\cos i. \tag{31}$$

Following the procedure outlined in §2.1 and detailed in Appendix B, the short-periodic perturbations in the eccentricity vector, angular momentum vector, and mean longitude can be stated as

$$\boldsymbol{e}^{sp}(t) = -\frac{3J_2 R^2}{2p^2}\left\{\left[\widehat{I}_2 + 2(I_1 + eII_{11} + III_{111} - III_{122} - 5IV_{122})(\hat{\boldsymbol{e}}\cdot\hat{\boldsymbol{p}})(\hat{\boldsymbol{e}}_\perp\cdot\hat{\boldsymbol{p}})\right.\right.$$
$$\left.- (2\widehat{III}_{112} + 5\widehat{IV}_{112})(\hat{\boldsymbol{e}}\cdot\hat{\boldsymbol{p}})^2 + (2\widehat{I}_2 + 2e\widehat{II}_{12} + 2\widehat{III}_{112} - 5\widehat{IV}_{222})(\hat{\boldsymbol{e}}_\perp\cdot\hat{\boldsymbol{p}})^2\right]\hat{\boldsymbol{e}}$$
$$- \left[I_1 - Me + 2(\widehat{I}_2 - e\widehat{II}_{12} - \widehat{III}_{112} + \widehat{III}_{222} - 5\widehat{IV}_{112})(\hat{\boldsymbol{e}}\cdot\hat{\boldsymbol{p}})(\hat{\boldsymbol{e}}_\perp\cdot\hat{\boldsymbol{p}})\right.$$
$$\left.+ (3Me/2 + 2I_1 + 2III_{122} - 5IV_{111})(\hat{\boldsymbol{e}}\cdot\hat{\boldsymbol{p}})^2 + (3Me/2 - 2eII_{22} - 2III_{122} - 5IV_{122})(\hat{\boldsymbol{e}}_\perp\cdot\hat{\boldsymbol{p}})^2\right]\hat{\boldsymbol{e}}_\perp$$
$$\left.+ Me(\hat{\boldsymbol{e}}_\perp\cdot\hat{\boldsymbol{p}})(\hat{\boldsymbol{h}}\cdot\hat{\boldsymbol{p}})\hat{\boldsymbol{h}} - 2e\left[\widehat{II}_{12}(\hat{\boldsymbol{e}}\cdot\hat{\boldsymbol{p}}) + II_{22}(\hat{\boldsymbol{e}}_\perp\cdot\hat{\boldsymbol{p}})\right]\hat{\boldsymbol{p}}\right\}, \tag{32a}$$

$$\boldsymbol{H}^{sp}(t) = -\frac{3HJ_2 R^2}{p^2}\left\{\left[\widehat{II}_{12}(\hat{\boldsymbol{e}}\cdot\hat{\boldsymbol{p}})(\hat{\boldsymbol{h}}\cdot\hat{\boldsymbol{p}}) + (II_{22} - M/2)(\hat{\boldsymbol{e}}_\perp\cdot\hat{\boldsymbol{p}})(\hat{\boldsymbol{h}}\cdot\hat{\boldsymbol{p}})\right]\hat{\boldsymbol{e}}$$

$$- \Big[(II_{11} - M/2)(\hat{\boldsymbol{e}} \cdot \boldsymbol{p})(\hat{\boldsymbol{h}} \cdot \boldsymbol{p}) + \widehat{II}_{12}(\hat{\boldsymbol{e}}_\perp \cdot \boldsymbol{p})(\hat{\boldsymbol{h}} \cdot \boldsymbol{p}) \Big] \hat{\boldsymbol{e}}_\perp$$

$$+ \Big[II_{11} - II_{22} + \widehat{II}_{12} \left((\hat{\boldsymbol{e}}_\perp \cdot \boldsymbol{p})^2 - (\hat{\boldsymbol{e}} \cdot \boldsymbol{p})^2 \right) \Big] \hat{\boldsymbol{h}} \Big\}, \tag{32b}$$

$$l^{sp}(t) = \frac{3J_2 R^2}{2p^2} \Bigg\{ \frac{e}{1 + \sqrt{1 - e^2}} \Big[I_1 - 3 \Big(IV_{111}(\hat{\boldsymbol{e}} \cdot \boldsymbol{p})^2 + 2\widehat{IV}_{112}(\hat{\boldsymbol{e}} \cdot \boldsymbol{p})(\hat{\boldsymbol{e}}_\perp \cdot \boldsymbol{p}) + IV_{122}(\hat{\boldsymbol{e}}_\perp \cdot \boldsymbol{p})^2 \Big)$$

$$+ 2 \left(\widehat{III}_{222} - \widehat{III}_{112} + \widehat{IV}_{222} - \widehat{IV}_{112} \right) (\hat{\boldsymbol{e}} \cdot \boldsymbol{p})(\hat{\boldsymbol{e}}_\perp \cdot \boldsymbol{p}) + 2 \left(III_{122} + IV_{122} \right) \left((\hat{\boldsymbol{e}} \cdot \boldsymbol{p})^2 - (\hat{\boldsymbol{e}}_\perp \cdot \boldsymbol{p})^2 \right) \Big]$$

$$- 2 \left(3\sqrt{1 - e^2} + \frac{\hat{\boldsymbol{h}} \cdot \boldsymbol{p}}{1 + \hat{\boldsymbol{h}} \cdot \boldsymbol{p}} \right) \left(II_{11}(\hat{\boldsymbol{e}} \cdot \boldsymbol{p})^2 + 2\widehat{II}_{12}(\hat{\boldsymbol{e}} \cdot \boldsymbol{p})(\hat{\boldsymbol{e}}_\perp \cdot \boldsymbol{p}) + II_{22}(\hat{\boldsymbol{e}}_\perp \cdot \boldsymbol{p})^2 \right) + 2\sqrt{1 - e^2} I_0$$

$$- \frac{1}{2} M \left[\sqrt{1 - e^2} \left(3(\hat{\boldsymbol{h}} \cdot \boldsymbol{p})^2 - 1 \right) + 5(\hat{\boldsymbol{h}} \cdot \boldsymbol{p})^2 - 2(\hat{\boldsymbol{h}} \cdot \boldsymbol{p}) - 1 \right]$$

$$+ \frac{3eH}{np^2} \sqrt{1 - e^2} \Big[2 \left(\widetilde{IV} + e\widetilde{II} \right)(\hat{\boldsymbol{e}} \cdot \boldsymbol{p})(\hat{\boldsymbol{e}}_\perp \cdot \boldsymbol{p}) + \widehat{\widetilde{I}}_2 \left(1 + 2(\hat{\boldsymbol{e}}_\perp \cdot \boldsymbol{p})^2 \right)$$

$$- 5\widehat{\widetilde{IV}}_{112}(\hat{\boldsymbol{e}} \cdot \boldsymbol{p})^2 - 5\widehat{\widetilde{IV}}_{222}(\hat{\boldsymbol{e}}_\perp \cdot \boldsymbol{p})^2 - 2 \left(\widehat{\widetilde{III}}_{112} + e\widehat{\widetilde{II}}_{12} \right) \left((\hat{\boldsymbol{e}} \cdot \boldsymbol{p})^2 - (\hat{\boldsymbol{e}}_\perp \cdot \boldsymbol{p})^2 \right) \Big]$$

$$+ \frac{6H}{np^2} (1 - e^2)^{3/2} \Big[\widetilde{II}(\hat{\boldsymbol{e}} \cdot \boldsymbol{p})(\hat{\boldsymbol{e}}_\perp \cdot \boldsymbol{p}) - \widehat{\widetilde{II}}_{12} \left((\hat{\boldsymbol{e}} \cdot \boldsymbol{p})^2 - (\hat{\boldsymbol{e}}_\perp \cdot \boldsymbol{p})^2 \right) \Big] \Bigg\}, \tag{32c}$$

where Roman numerals I_1, I_2, II_{11}, ... designate various functions of true anomaly, $\widehat{I}_2$, $\widehat{II}_{12}$, ... represent the difference of these trigonometric expressions from their averaged values, $\widetilde{I}_1$, ... are indefinite integrals of the previous core functions, and $\widehat{\widetilde{I}}_2$, ..., represent differences between the doubly-integrated expressions, their averaged values, and the previous core averages. While somewhat cumbersome, the adopted notation mirrors the derivation of Appendix B and is otherwise systematic and methodical. The needed results pertaining to the solution, Eq. (32), are given by

$$I_0 = f + e \sin f, \tag{33a}$$

$$I_1 = \frac{1}{12} \left(12ef + (12 + 9e^2) \sin f + 6e \sin 2f + e^2 \sin 3f \right), \tag{33b}$$

$$II_{11} = \frac{1}{12} \left(6f + 9e \sin f + 3 \sin 2f + e \sin 3f \right), \tag{33c}$$

$$II_{22} = \frac{1}{12} \left(6f + 3e \sin f - 3 \sin 2f - e \sin 3f \right), \tag{33d}$$

$$III_{111} = \frac{1}{96} \left(36ef + 72 \sin f + 24e \sin 2f + 8 \sin 3f + 3e \sin 4f \right), \tag{33e}$$

$$III_{122} = \frac{1}{96} \left(12ef + 24 \sin f - 8 \sin 3f - 3e \sin 4f \right), \tag{33f}$$

$$IV_{111} = \frac{1}{240} \left(180ef + 30(6 + 5e^2) \sin f + 120e \sin 2f + 5(4 + 5e^2) \sin 3f + 15e \sin 4f + 3e^2 \sin 5f \right), \tag{33g}$$

$$IV_{122} = \frac{1}{240} \left(60ef + 30(2 + e^2) \sin f - 5(4 + e^2) \sin 3f - 15e \sin 4f - 3e^2 \sin 5f \right), \tag{33h}$$

$$\widehat{I}_2 = -\frac{1}{12} \left((12 + 3e^2)(\cos f - X_0^{0,1}) + 6e(\cos 2f - X_0^{0,2}) + e^2(\cos 3f - X_0^{0,3}) \right), \tag{34a}$$

$$\widehat{II}_{12} = -\frac{1}{12} \left(3e(\cos f - X_0^{0,1}) + 3(\cos 2f - X_0^{0,2}) + e(\cos 3f - X_0^{0,3}) \right), \tag{34b}$$

$$\widehat{III}_{112} = -\frac{1}{96} \left(24(\cos f - X_0^{0,1}) + 12e(\cos 2f - X_0^{0,2}) + 8(\cos 3f - X_0^{0,3}) + 3e(\cos 4f - X_0^{0,4}) \right), \tag{34c}$$

$$\widehat{III}_{222} = -\frac{1}{96} \left(72(\cos f - X_0^{0,1}) + 12e(\cos 2f - X_0^{0,2}) - 8(\cos 3f - X_0^{0,3}) - 3e(\cos 4f - X_0^{0,4}) \right), \tag{34d}$$

$$\widehat{IV}_{112} = -\frac{1}{240} \left(30(2 + e^2)(\cos f - X_0^{0,1}) + 60e(\cos 2f - X_0^{0,2}) + 5(4 + 3e^2)(\cos 3f - X_0^{0,3}) \right.$$
$$\left. + 15e(\cos 4f - X_0^{0,4}) + 3e^2(\cos 5f - X_0^{0,5}) \right), \tag{34e}$$

$$\widehat{IV}_{222} = -\frac{1}{240} \left(30(6 + e^2)(\cos f - X_0^{0,1}) + 60e(\cos 2f - X_0^{0,2}) - 5(4 - e^2)(\cos 3f - X_0^{0,3}) \right.$$
$$\left. - 15e(\cos 4f - X_0^{0,4}) - 3e^2(\cos 5f - X_0^{0,5}) \right), \tag{34f}$$

$$\widehat{\widehat{I}}_2 = -\frac{1}{12} \sum_{k=1}^{\infty} \frac{1}{k} \left((12 + 3e^2)C_k^{0,1} + 6eC_k^{0,2} + e^2 C_k^{0,3} \right) \sin kM, \tag{35a}$$

$$\widehat{\widehat{II}}_{12} = -\frac{1}{12} \sum_{k=1}^{\infty} \frac{1}{k} \left(3eC_k^{0,1} + 3C_k^{0,2} + eC_k^{0,3} \right) \sin kM, \tag{35b}$$

$$\widehat{\widehat{\widehat{III}}}_{112} = -\frac{1}{96} \sum_{k=1}^{\infty} \frac{1}{k} \left(24C_k^{0,1} + 12eC_k^{0,2} + 8C_k^{0,3} + 3eC_k^{0,4} \right) \sin kM, \tag{35c}$$

$$\widehat{\widehat{IV}}_{112} = -\frac{1}{240} \sum_{k=1}^{\infty} \frac{1}{k} \left(30(2 + e^2)C_k^{0,1} + 60eC_k^{0,2} + 5(4 + 3e^2)C_k^{0,3} + 15eC_k^{0,4} + 3e^2 C_k^{0,5} \right) \sin kM, \tag{35d}$$

$$\widehat{\widehat{IV}}_{222} = -\frac{1}{240} \sum_{k=1}^{\infty} \frac{1}{k} \left(30(6 + e^2)C_k^{0,1} + 60eC_k^{0,2} - 5(4 - e^2)C_k^{0,3} - 15eC_k^{0,4} - 3e^2 C_k^{0,5} \right) \sin kM, \tag{35e}$$

$$\widetilde{\mathcal{II}} = -\frac{1}{6} \sum_{k=1}^{\infty} \frac{1}{k} \left(3eS_k^{0,1} + 3S_k^{0,2} + eS_k^{0,3} \right) \cos kM, \tag{36a}$$

$$\widetilde{\mathcal{IV}} = -\frac{1}{48} \left[\sum_{k=1}^{\infty} \frac{1}{k} \left(6(2 + e^2)S_k^{0,1} + 36eS_k^{0,2} + (28 + 9e^2)S_k^{0,3} + 18eS_k^{0,4} + 3e^2 S_k^{0,5} \right) \cos kM \right], \tag{36b}$$

where all intermediate terms are given in Appendix B.

Thus, following Eq. (6), given the initial osculating state $(\boldsymbol{e}_0, \boldsymbol{H}_0, l_0)$, the mean equations of motion, Eqs. (30), have to be initialized as

$$\begin{cases} \overline{\boldsymbol{e}}_0 = \boldsymbol{e}_0 - \boldsymbol{e}^{sp}(t_0), \\ \overline{\boldsymbol{H}}_0 = \boldsymbol{H}_0 - \boldsymbol{H}^{sp}(t_0), \\ \bar{l}_0 = l_0 - l^{sp}(t_0). \end{cases} \tag{37}$$

4 Numerical comparisons with Brouwer-Lyddane

Lyddane (1963), in establishing the validity of his new formulas for small eccentricities and inclinations that leverages the fundamental solution of Brouwer (1959), made only a few comparisons with the results of a Cowell integration. The general domain of validity of the Brouwer-Lyddane (BL) mean-to-osculating theory, however, has hitherto not been established. Here, we consider an extended grid of initial conditions and test the developed Milankovitch formulation against both BL and the fully numerical transformation of §2.2. For Brouwer-Lyddane, we have verified that the more streamlined formulas presented in Schaub and Junkins (2018) have been correctly transcribed according to their original sources, excepting the missing $\sin(2\omega)$ factor in the long-period terms of M, ω, and Ω, which has only been noted in the recent erratum of the latest edition of this widely used monograph.[3] Furthermore, rather than using Lyddane's adhoc modification, Gim and Alfriend (2003) developed a new theory based on Brouwer's generating function that uses equinoctial elements. While still invalid at the critical inclination, Gim and Alfriend (2003) concluded from various numerical simulations that their method produces reasonable results within $0.25°$ of this small divisor. Being inherently rooted in Brouwer's theory, it was expected at the outset that Lyddane (1963) and Gim and Alfriend (2003) would yield the same overall degree of accuracy. Nevertheless, for the sake of completeness, and because, superficially, it is not apparent that the formulas of Gim and Alfriend (2003) are mathematically equivalent to those systematized in Schaub and Junkins (2018),[4] we have also extended our numerical campaign to include a comparison between these as well (see Appendix C).

Figure 2 shows a numerical confirmation of the validity of the Milankovitch formulation for satellites of the Sun-synchronous and Molniya type. The procedure was to first convert the initial osculating orbit into its corresponding mean elements using the developed formulas. These initial osculating and mean

---

[3] Retaining the long-periodic perturbations in the transformation from osculating to mean elements is technically a misuse of Brouwer's theory (Breakwell and Vagners 1970); yet, it is, perhaps inadvertently, done in the literature (Schaub and Alfriend 2001) and we show herein that it does not have much bearing on the solutions outside the critical inclination.

[4] We have verified that the expressions for a and i do indeed agree, but have not done so for the remaining elements, which is a more painstaking and arduous task.

states were then propagated according to their dynamics described by Eqs. (29) and (30). In the former case, the results are equivalent to, though generally more accurate than, a simple Cowell integration in Cartesian space. The time histories of these evolutions at various subintervals were subsequently used as input to the respective osculating-to-mean and mean-to-osculating transformations in order to recover the aforementioned simulated trajectories.
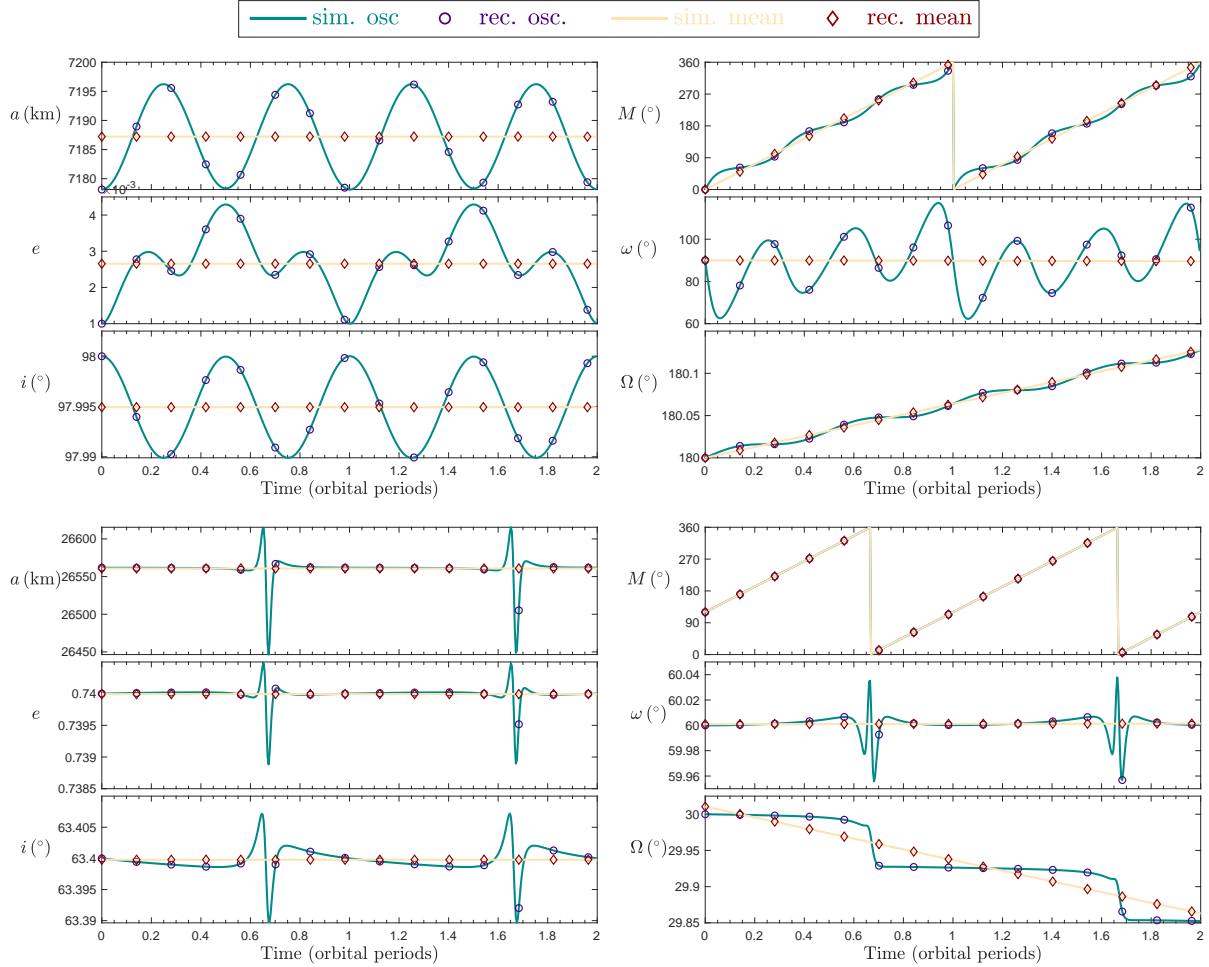

Fig. 2 Evolution of the osculating and mean orbital elements for a low-altitude, nearly circular, and retrograde satellite (*top*) and a highly elliptical, semi-synchronous, critically inclined satellite (*bottom*). The initial osculating states $(a, e, i, M, \omega, \Omega) = (R + 800 \, \text{km}, 0.001, 98°, 0, 90°, 180°)$ (*top*) and $(26562 \, \text{km}, 0.74, 64.3°, 120°, 60°, 30°)$ (*bottom*) were converted into their corresponding mean elements using the developed Milankovitch formulation, and each set was propagated according to Eqs. (29) and (30), respectively. The osculating (*cyan*) and mean (*yellow*) trajectories were recovered (*purple circles* and *red diamonds*) at equal time steps using the aforementioned transformations, taking the respective simulated dynamics as input.

Projecting both the simulated and recovered osculating evolutions into the radial, along-track, and cross-track frame, we use the norm root mean square (RMS) of the positional error as a means to assess the accuracy of the transformation. To keep the presentation brief, we do not consider the velocity errors or other metrics. Figure 3 shows the results of this process for Brouwer-Lyddane, Milankovitch, and the numerical transformations, respectively, for Sun-synchronous-like orbits and nearly critically inclined, semi-synchronous ones. While the Milankovitch scheme yields sub-kilometer accuracy in these orbital configurations, neither BL nor the numerical formulation can handle the more challenging scenario. The dependence of the resulting errors on the choice of orbit orientation angles is also highlighted by Fig. 3.

For completeness and further validation, Figure 4 compares the aforementioned Brouwer-Lyddane transformation which includes the long-period terms, with a BL mean-to-osculating implementation that omits them. These test cases are simulated in the trusted semi-analytical propagator, STELA, using a J_2-only model. While slight discrepancies with STELA are to be expected due to different platforms, mean-element
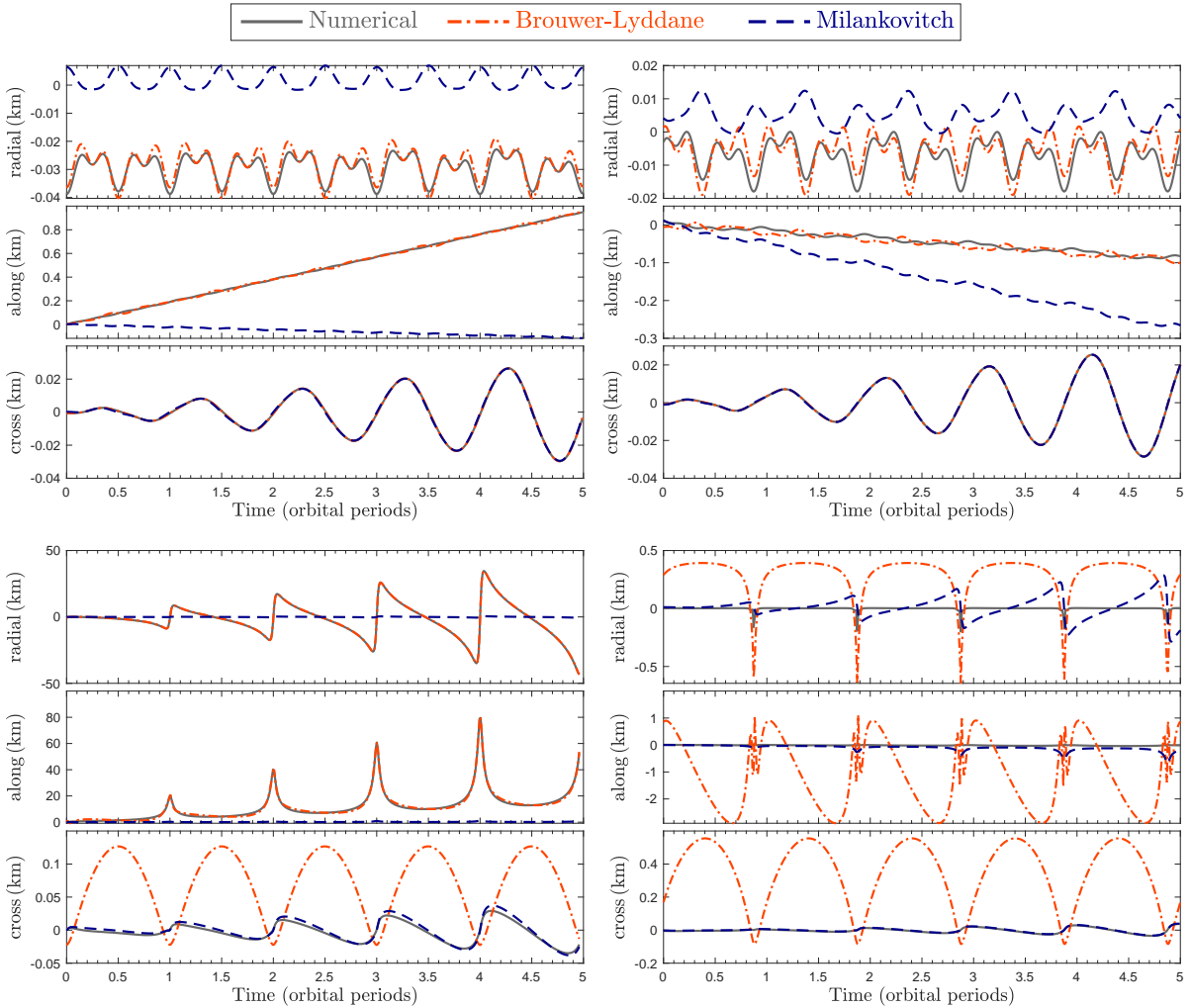
Fig. 3 Radial, along-track, and cross-track errors between the recovered and simulated osculating trajectories, using the Brouwer-Lyddane (*orange, dash-dot*), Milankovitch (*blue, dashed*), and numerical (*gray, solid*) transformations, respectively. The initial osculating orbits $(a, e, i) = (R + 800 \, \text{km}, 0.001, 98°)$ (*top*) and $(26562 \, \text{km}, 0.75, 63°)$ (*bottom*), each with $(\omega, \Omega) = (90°, 180°)$ and $M = 0$ (*left*) or $M = 45°$ (*right*), were converted to their corresponding mean states using each respective transformation and subsequently propagated following Eq. 30. At every time step, the simulated mean trajectory was converted to osculating according to each transformation and compared against the simulated dynamics of Eq. 29. The norm RMS of the difference between the recovered and simulated positions (in km) over five orbital periods varied between 0.0556 and 20.9714 for Brouwer-Lyddane, 0.0666 and 0.3114 for Milankovitch, and 0.0533 and 20.9796 for the numerical transformation.

equations, and astronomical constants used in the respective simulations, the results are in good quantitative agreement. Importantly, the long-period terms in the full Brouwer theory do not cause appreciable changes in the recovered solutions throughout the whole of orbital phase space excepting a narrow band centered around the critical inclination.

Figure 5 shows error maps corresponding to two different initial eccentricities for 500×500 grids of initial inclinations and semi-major axes. Each grid point, together with $(M, \omega, \Omega) = (0, 0, 0)$, was used to form the full osculating element state vector, and propagated for five orbital periods. The same procedure outlined in the previous paragraph was used to characterize the accuracy of each transformation, where the colorbar in Fig. 5 corresponds to the norm RMS of the difference between the recovered and simulated positions over the timescale of the propagations (five orbital periods). Note that prescribed limits were imposed on the colorbar of each map in this numerical campaign so as to more clearly highlight the differences among the various transformations.

For the low-Earth orbit (LEO) map of Fig. 5, for which $a \in (R + 200, R + 2000)$ km and $e = 0.01$, all three transformations performed worse for low inclinations, with the Milankovitch scheme slightly degrading at very low altitudes. Milankovitch has the highest accuracy near the critical inclination and its retrograde
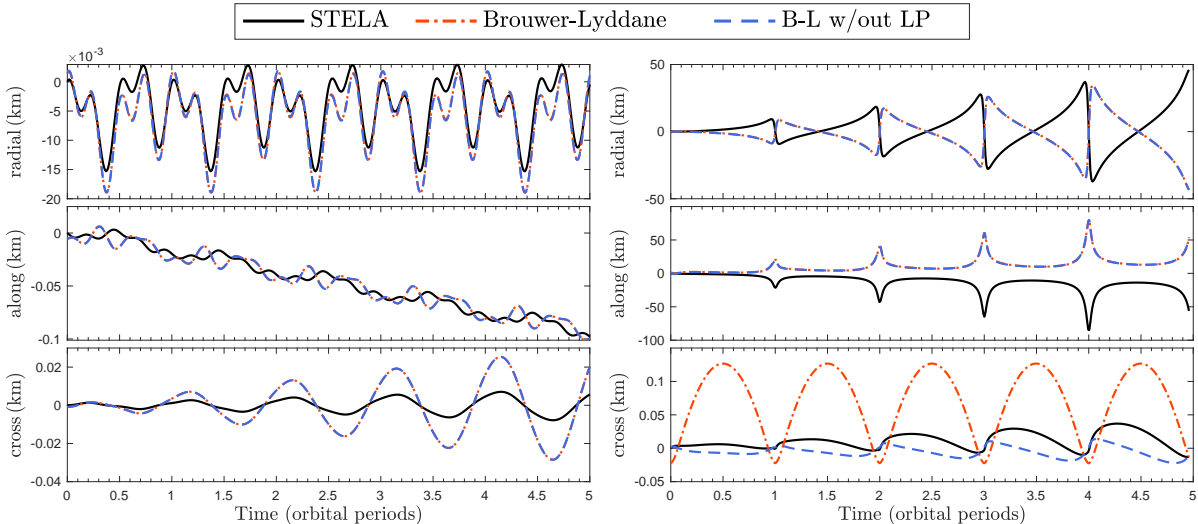
11

Fig. 4 Radial, along-track, and cross-track errors between the recovered and simulated osculating trajectories, using the full Brouwer-Lyddane (*orange, dash-dot*), BL without long-period terms (*blue, dashed*), and STELA (*black, solid*) transformations, respectively. The initial osculating orbits $(a, e, i) = (R + 800\,\text{km}, 0.001, 98°)$ (*left*) and $(26562\,\text{km}, 0.75, 63°)$ (*right*), each with $(\omega, \Omega) = (90°, 180°)$ and $M = 45$ (*left*) or $M = 0°$ (*right*), were converted to their corresponding mean states using each respective transformation and subsequently propagated. At every time step, the simulated mean trajectory was converted to osculating according to each transformation and compared against the simulated osculating dynamics. The norm RMS of the difference between the recovered and simulated positions (in km) over five orbital periods was 0.0556 and 20.9714 for BL, 0.0555 and 20.9785 for BL w/out LP, and 0.0543 and 22.4028 for the STELA transformation.

counterpart, while BL fails in these regimes.[5] The Milankovitch transformation has a similar high performance as the numerical scheme for the medium-Earth orbit (MEO) to geosynchronous orbit (GEO) map, which considers a higher initial osculating eccentricity of $e = 0.2$. For even higher eccentricities, however, as in those considered in the geostationary-transfer orbit (GTO) and Molniya maps of Fig. 6, both the BL and the numerical schemes break down. Brouwer-Lyddane is particularly divergent within the band centered at the critical inclination, as expected, but otherwise yielded similarly poor results as the numerical transformation.

Figure 7 shows error maps in the semi-major axis–eccentricity plane for four different initial inclinations. For all three transformations, the error is highest at the boundary of allowable orbits, above which the perigee altitude would equal the Earth's radius. Only the Milankovitch formulation can accurately treat all permissible initial conditions of these maps. The retrograde critical inclination map sheds more light on the intrinsic singularity present in BL, which often leads to unphysical results.

The remaining slice of the action-like element space is given in Fig. 8, which shows how the errors manifest in the (i, e) plane for two values of initial semi-major axes (representing LEO satellites at 800 km altitude and GEO birds). Once again, we can see that Milankovitch is somewhat weak in the low-inclination, low-eccentricity, and low-altitude regimes, but otherwise can adequately treat all of phase space, including orbits near the critical inclination that render BL singular and the high-eccentricity orbits that cause issues in the numerical transformation. The reason for the slight degradation in performance of Milankovitch remains unknown.

It must be noted that all previous error maps were constructed with the same set of orbital angles M, ω, and Ω (all being set to zero). As shown earlier in Fig. 3, other specific combinations of angles lead to different evolutions, in general, and different error residuals. Figure 9 shows how such errors manifest in the angles phase space for a particular set of (a, e, i). While not readily apparent in the Milankovitch transformation, Brouwer's theory has no functional dependence on Ω, and thus the errors are expected to be independent of this orientation angle. This is validated in Fig 9, where we can also see that the errors in both the BL and numerical solutions spike at $M + \omega = 90°$. Strikingly, this specific value of mean argument of latitude is when Milankovitch performs best. It can be concluded from Fig 9 that setting all angles to zero did not unfairly bias any of the previous error map results.

---

[5] Note that neither an implementation of BL without the long-period terms or STELA would be singular here, but would otherwise perform as the numerical scheme (cf., e.g., Figs. 3 and 4).
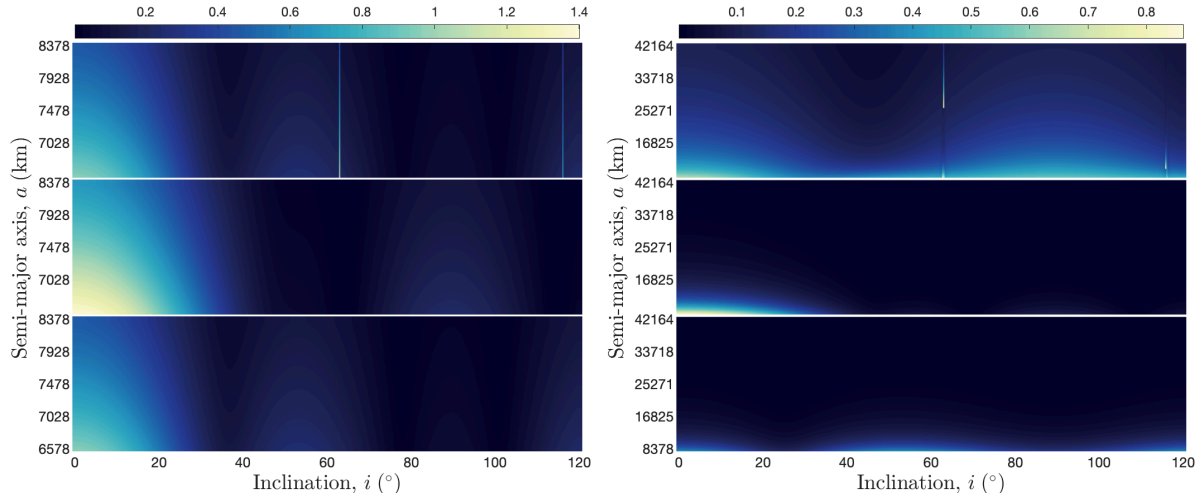
Fig. 5 Error maps in the inclination–semi-major axis plane using the Brouwer-Lyddane (*top*), Milankovitch (*middle*), and numerical (*bottom*) transformations, respectively. Each panel samples an equidistant grid of 250 thousand initial osculating (i, a) values, for initial eccentricities of 0.01 (*left*) and 0.2 (*right*), and where the initial mean anomaly, perigee, and node angles were all set to zero. The colorbar represents the norm RMS of the difference between the recovered and simulated positions over five orbital periods, according to each formulation. The colorbar limit was set to the maximum error found between the Milankovitch and numerical schemes, as the Brouwer-Lyddane formulation becomes singular near the critical inclination. Grid points leading to unphysical errors or to values that exceed this limit are represented in *white*. From *left* to *right*, the *(maximum, mean)* errors (in km) were $(1.0626, 0.1967)$ and $(68.9371, 0.1804)$ for Brouwer-Lyddane, $(1.4004, 0.2664)$ and $(0.8627, 0.0268)$ for Milankovitch, and $(0.9673, 0.1933)$ and $(0.3948, 0.0334)$ for the numerical scheme.
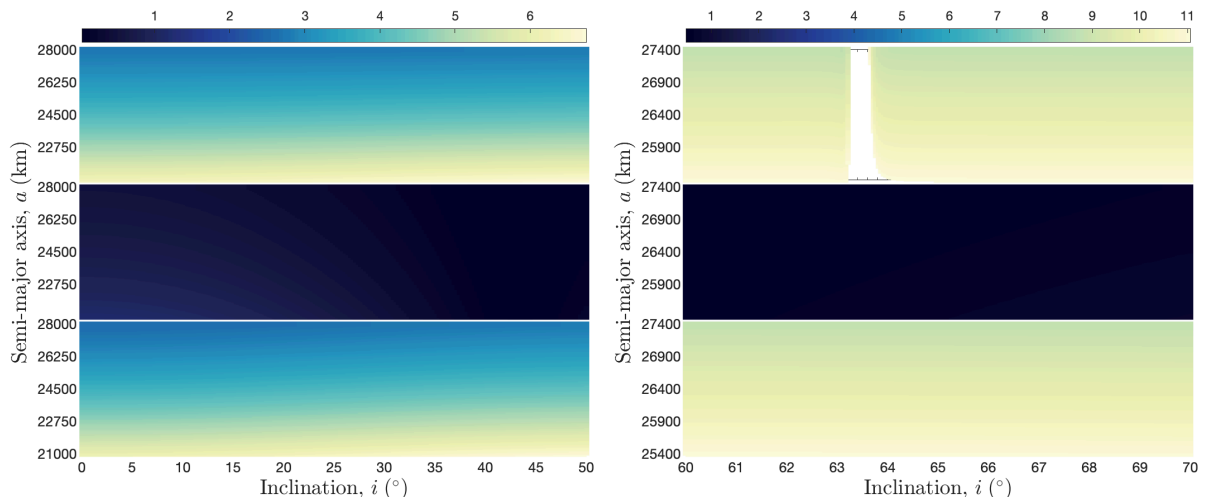

Fig. 6 Error maps in the inclination–semi-major axis plane using the Brouwer-Lyddane (*top*), Milankovitch (*middle*), and numerical (*bottom*) transformations, respectively. Each panel samples an equidistant grid of 40 thousand initial osculating (i, a) values, for initial eccentricities of 0.69 (*left*) and 0.74 (*right*), and where the initial mean anomaly, perigee, and node angles were all set to zero. The colorbar represents the norm RMS of the difference between the recovered and simulated positions over five orbital periods, according to each formulation. The colorbar limit was set to the maximum error found between the Milankovitch and numerical schemes, as the Brouwer-Lyddane formulation becomes singular near the critical inclination. Grid points leading to unphysical errors or to values that exceed this limit are represented in *white*. From *left* to *right*, the *(maximum, mean)* errors (in km) were $(6.7332, 4.3022)$ and $(1689.0290, 19.5805)$ for Brouwer-Lyddane, $(1.1909, 0.4257)$ and $(0.8106, 0.6340)$ for Milankovitch, and $(6.7502, 4.2019)$ and $(11.0569, 9.8514)$ for the numerical scheme.

5 Discussion

Appendix C provides a detailed comparison of Brouwer-Lyddane against Gim-Alfriend (GA), the implementations of both contain the long-period terms. While still suffering from the critical inclination singularity, the formulas of Gim and Alfriend (2003) yield a more consistent result, on average, with the numerical scheme. This is surprising given that they were both fundamentally based on the same generating function, given by Brouwer (1959), and the modifications made by Lyddane (1963) also rendered the solution valid
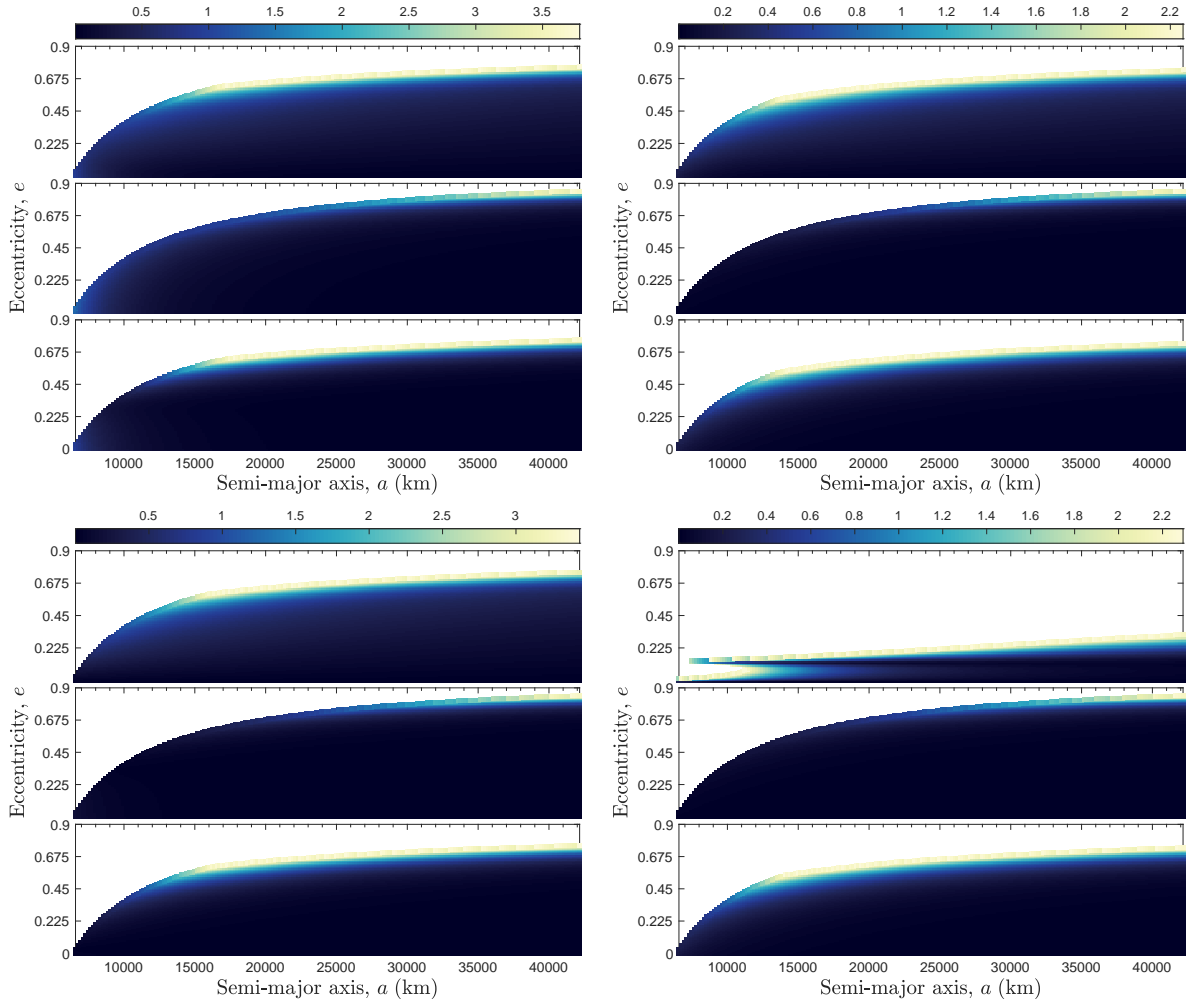
Fig. 7 Error maps in the semi-major axis–eccentricity plane using the Brouwer-Lyddane (*top* panels), Milankovitch (*middle* panels), and numerical (*bottom* panels) transformations, respectively. Each panel samples an equidistant grid of 40 thousand initial osculating (a, e) values, for initial inclinations of $6°$ (*top-left*), $63°$ (*top-right*), $98°$ (*bottom-left*), and $116.6°$ (*bottom-right*), and where the initial mean anomaly, perigee, and node angles were all set to zero. The colorbar represents the norm RMS of the difference between the recovered and simulated positions over five orbital periods, according to each formulation. The colorbar limit of each map was set to the maximum error found in the Milankovitch scheme to provide a better contrast. Grid points leading to unphysical errors or to values that exceed this limit are represented in *white*. Clockwise starting from the *top left*: Brouwer-Lyddane recorded *(maximum, mean)* errors (in km) of $(58.5237, 1.2662)$, $(59.5538, 1.2013)$, $(59.6549, 1.2698)$, and $(82198.6187, 218.0410)$; Milankovitch recorded errors of $(3.7776, 0.2221)$, $(2.2572, 0.0675)$, $(3.4344, 0.0914)$, and $(2.2940, 0.0682)$; and the numerical scheme recorded errors of $(58.4914, 1.0276)$, $(59.5997, 1.1049)$, $(59.5904, 1.0825)$, and $(59.6009, 1.1046)$.

for small eccentricities and inclinations. Nevertheless, while notable quantitative differences are apparent in Appendix C, they are in good qualitative agreement, though neither can adequately treat orbits near the critical inclination or those of high eccentricity.

Being a non-canonical set of elements, our derivation followed the approach used by Kozai (1959), as further elucidated by Scheeres (2012). We note, however, that, like Gim and Alfriend (2003), we could have merely adopted Brouwer's generating function and computed the short-periodic corrections using Poisson-bracket operations. Nevertheless, we elected to present an independent derivation on account of the numerical results of Appendix C, and because our future work will extend our formulation to other perturbations for which a convenient generating function is not always available Shen et al (2019).

~~Aksnes (1972) reformulated Brouwer's first-order theory in terms of the Hill variables, which freed it of the mathematical singularities associated with circular or equatorial orbits, but his approach is still plagued by the unwieldy critical divisor $1 - 5\cos^2 i$ that, states Aksnes, "will, of course, appear regardless of which variables are used."~~ Our Milankovitch formulation is closed-form in both e and H, and we have provided a general series solution for the mean longitude l based on Hansen coefficients that can be taken
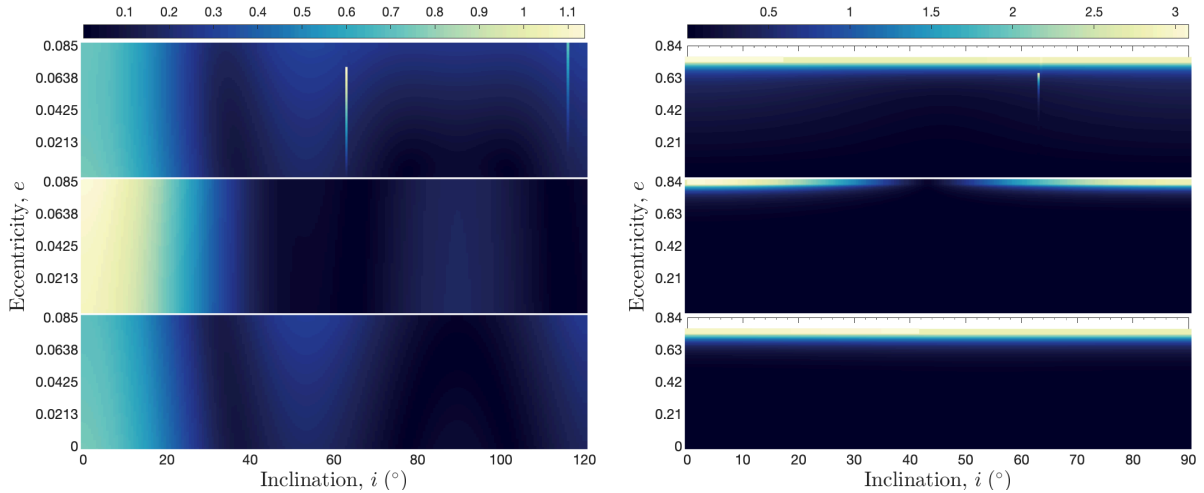
Fig. 8 Error maps in the inclination–eccentricity plane using the Brouwer-Lyddane (*top*), Milankovitch (*middle*), and numerical (*bottom*) transformations, respectively. Each panel samples an equidistant grid of 40 thousand initial osculating (i,a) values, for initial semi-major axes of $R+800$ km (*left*) and a_{GEO} (*right*), and where the initial mean anomaly, perigee, and node angles were all set to zero. The colorbar represents the norm RMS of the difference between the recovered and simulated positions over five orbital periods, according to each formulation. The colorbar limit of each map was set to the maximum error found in the Milankovitch scheme to provide a better contrast. Grid points leading to unphysical errors or to values that exceed this limit are represented in *white*. From *left* to *right*, the *(maximum, mean)* errors (in km) were $(1.2992, 0.2601)$ and $(94.1968, 1.9108)$ for Brouwer-Lyddane, $(1.1378, 0.2973)$ and $(3.0803, 0.0955)$ for Milankovitch, and $(0.7508, 0.2230)$ and $(45.3521, 1.7884)$ for the numerical scheme.
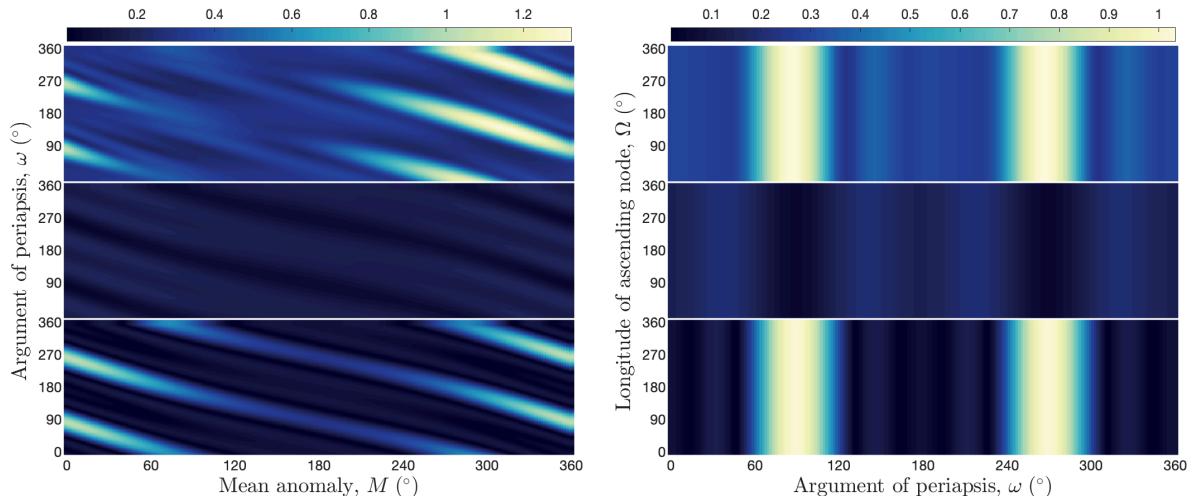

Fig. 9 Error maps in the mean anomaly–periapsis angle plane (*left*) and periapsis–node angles plane (*right*) using the Brouwer-Lyddane (*top*), Milankovitch (*middle*), and numerical (*bottom*) transformations, respectively. Each panel samples an equidistant grid of 40 thousand initial osculating (M,ω) or (ω,Ω) values, for an initial semi-major axis of $R+800$ km (*left*), eccentricity of 0.1, and inclination of 98°. The remaining orbital element needed to form the full state vector was set to zero in each case. The colorbar represents the norm RMS of the difference between the recovered and simulated positions over five orbital periods, according to each formulation. The colorbar limit was set to the maximum error found across all schemes, as there were no singular or outlier cases for these maps. From *left* to *right*, the *(maximum, mean)* errors (in km) were $(1.3241, 0.4100)$ and $(1.0332, 0.4704)$ for Brouwer-Lyddane, $(0.2068, 0.1417)$ and $(0.2064, 0.1490)$ for Milankovitch, and $(1.0182, 0.2048)$ and $(1.0180, 0.3181)$ for the numerical scheme.

to any desired order of accuracy.[6] Although not leading to drastic errors, improvements should be sought in our algorithm for treating low-altitude orbits of small eccentricity and inclinations, as this is the only orbital regime for which Milankovitch did not outperform the rest. We note that our formulation bypasses the critical inclination because we do not consider the long-periodic terms that arise from a second-order

---

[6] Truncating to order 12 in the Hansen coefficients was found to yield accurate results, in general, with higher orders being needed with increasing eccentricity.

perturbation treatment. On this account, we also omitted these in Brouwer's theory in Fig. 4 to compare the performance against our ~~solely first-order~~ vectorial formulation. We emphasize that the long-periodic terms included in the recovered solutions for BL and GA for all presented error maps are otherwise negligible away from the critical inclination.

6 Conclusions

We have developed a new mean-to-osculating and inverse transformation based on the Milankovitch vectorial elements and with the mean longitude as the fast variable, that is valid for all eccentricity less than one. An extensive numerical campaign was used to validate the vectorial transformation over orbital phase-space grids tailored to the relative distribution of cataloged Earth satellites and debris. Having provided a general Kozai-like scheme, not rooted in canonical perturbation theory, our approach can be adopted to nonconservative forces, such as solar radiation pressure and atmospheric drag, in addition to treating lunisolar third-body gravity and other predominant perturbations (Shen et al 2019). It could also be advantageous to use the true orbit longitude as the fast variable, given that the non-averaged and averaged equations are more simple than those for the mean longitude.

A Auxiliary Formulas

We require the double quadrature of f, $\sin mf$, $\cos mf$, where m is an integer. The traditional approach has resorted to more or less elaborate expansions of various functions into sums of periodic terms, which depend chiefly on Taylor's series and Fourier's theorem, mainly because the integrals of these functions cannot be obtained conveniently in any other way (Brumberg 1995). While detailed explicit tabulations for these quantities may be found in Cayley's and Newcomb's classical tables, these results may be deduced from the Hansen coefficients (Hughes 1981). Namely,

$$\sin mf = \sum_{k=1}^{\infty} S_k^{0,m}(e) \sin kM, \tag{38a}$$

$$\cos mf = C_0^{0,m}(e) + \sum_{k=1}^{\infty} C_k^{0,m}(e) \cos kM, \tag{38b}$$

where the coefficients $S_k^{n,m}$ and $C_k^{n,m}$ for integers k, n, and m are power series in the eccentricity, starting with degree $|m-k|$, and are related to Hansen coefficients $X_k^{n,m}$ by

$$C_0^{n,m} = X_0^{n,m}, \tag{39}$$
$$C_k^{n,m} = X_k^{n,m} + X_{-k}^{n,m}, \tag{40}$$
$$S_k^{n,m} = X_k^{n,m} - X_{-k}^{n,m}. \tag{41}$$

For $k = 0$, exact analytical expressions exist for the zero-order Hansen coefficients $X_0^{n,m}$ for all values of n and m; in particular, we recall a special result for the zero-order Hansen coefficients, derived by Kozai (1962a):

$$X_0^{0,m} = \frac{1}{2\pi} \int_0^{2\pi} \cos(mf)\, \mathrm{d}M = \frac{(-e)^m(1 + m\sqrt{1-e^2})}{(1+\sqrt{1-e^2})^m}, \qquad m = 1, 2, 3, \ldots \tag{42}$$

For $k \neq 0$, the analytical expressions for them do not terminate and, consequently, the series have to be truncated at some particular order in the eccentricity.

Hansen's coefficients can be expressed as series invoking Bessel and hypergeometric functions from which several formulae of recurrence can be derived that greatly facilitate their calculation (Challe and Laclaverie 1969; Giacaglia 1976):

$$kX_k^{n,m} = \frac{ne}{2\eta}\left(X_k^{n-1,m-1} - X_k^{n-1,m+1}\right) + m\eta X_k^{n-2,m}, \tag{43}$$

16

$$(1-e^2)^2 X_k^{n,m} = \left(1 - \frac{e^2}{2}\right) X_k^{n+2,m} + e(1-e^2)\left(X_k^{n+1,m+1} + X_k^{n+1,m-1}\right) - \frac{e^2}{4}\left(X_k^{n+2,m+2} + X_k^{n+2,m-2}\right).$$

(44)

A useful series representation to seed the recursion, which dates back to Hansen, is given by (Proulx and McClain 1988)

$$X_k^{n,m} = (1+\beta^2)^{-(n+1)}(-\beta)^{|k-m|}\sum_{\ell=0}^{\infty} L_{\ell+s}^{(n-m-\ell-s-1)}\left(k\sqrt{1+\beta^2}\right) L_{\ell+t}^{(a+m-\ell-t-1)}\left(k\sqrt{1+\beta^2}\right)\beta^{2\ell}, \quad (45)$$

where the functions $L_i^{(j)}(x)$ are the generalized Laguerre polynomial defined as

$$L_i^{(j)}(x) = \sum_{\ell=0}^{\infty}(-1)^\ell \binom{i+j}{i-l}\frac{x^\ell}{\ell!}, \quad (46)$$

and

$$s = [|k-m|+(k+m)]/2, \quad (47)$$
$$t = [|k-m|-(k+m)]/2. \quad (48)$$

In the preceding expressions, $\eta = \sqrt{1-e^2}$ and $\beta = (1-\eta)/e$.

Also needed in our derivation is the classical equation of the center, which is given by

$$f = M + 2\sum_{k=1}^{\infty}\frac{1}{k}\left[J_k(ke) + \sum_{n=1}^{\infty}\beta^n\left(J_{k-n}(ke) + J_{k+n}(ke)\right)\right]\sin kM,$$

$$= M + \sum_{k=1}^{\infty}\phi_k \sin kM, \quad (49)$$

where $J_k(x)$ are Bessel functions of the first kind.

B Derivation of the short-periodic perturbations in the Milankovitch elements

The procedure involves first writing down an approximate differential equation that governs the short-period dynamics for each variable (e, H, l), according to Eq. (4). The first indefinite time integration of Eq. (5) requires the quadrature of dyadics and higher rank tensors of the dynamical variable r. In particular, we can expose all of the fast-variable terms of Eq. (13), and can complete the needed core integrals by changing the dependent variable from time to true anomaly or mean anomaly:

$$dt = \frac{r^2}{H}df = \frac{1}{n}dM. \quad (50)$$

Specifically, we have

$$\int\frac{1}{r^3}dt = \frac{1}{H}\int\frac{1}{r}df$$
$$= \frac{\mu}{H^3}\int(1+e\cos f)df$$
$$= \frac{\mu}{H^3}I_0, \quad (51)$$

For the vector term, we have

$$I = \int\frac{\boldsymbol{r}}{r^5}dt = \frac{1}{H}\int\frac{\hat{\boldsymbol{r}}}{r^2}df$$
$$= \frac{\mu^2}{H^5}\int(1+e\cos f)^2(\cos f\hat{\boldsymbol{e}} + \sin f\hat{\boldsymbol{e}}_\perp)df$$
$$= \frac{\mu^2}{H^5}(I_1\hat{\boldsymbol{e}} + I_2\hat{\boldsymbol{e}}_\perp). \quad (52)$$

Similarly, for the dyadic terms, we find

$$II = \int \frac{\boldsymbol{rr}}{r^5}\,\mathrm{d}t = \frac{1}{H}\int \frac{\hat{\boldsymbol{r}}\hat{\boldsymbol{r}}}{r}\,\mathrm{d}f$$

$$= \frac{\mu}{H^3}\int (1 + e\cos f)\Big[\cos^2 f\,\hat{\boldsymbol{e}}\hat{\boldsymbol{e}} + \cos f\sin f(\hat{\boldsymbol{e}}\hat{\boldsymbol{e}}_\perp + \hat{\boldsymbol{e}}_\perp\hat{\boldsymbol{e}}) + \sin^2 f\,\hat{\boldsymbol{e}}_\perp\hat{\boldsymbol{e}}_\perp\Big]\,\mathrm{d}f$$

$$= \frac{\mu}{H^3}\Big[II_{11}\hat{\boldsymbol{e}}\hat{\boldsymbol{e}} + II_{12}(\hat{\boldsymbol{e}}\hat{\boldsymbol{e}}_\perp + \hat{\boldsymbol{e}}_\perp\hat{\boldsymbol{e}}) + II_{22}\hat{\boldsymbol{e}}_\perp\hat{\boldsymbol{e}}_\perp\Big], \tag{53}$$

where

$$II_{11} = \int (1 + e\cos f)\cos^2 f\,\mathrm{d}f$$

$$= \frac{1}{12}\Big(6f + 9e\sin f + 3\sin 2f + e\sin 3f\Big), \tag{54}$$

$$II_{12} = \int (1 + e\cos f)\cos f\sin f\,\mathrm{d}f$$

$$= -\frac{1}{12}\Big(3e\cos f + 3\cos 2f + e\cos 3f\Big), \tag{55}$$

$$II_{22} = \int (1 + e\cos f)\sin^2 f\,\mathrm{d}f$$

$$= \frac{1}{12}\Big(6f + 3e\sin f - 3\sin 2f - e\sin 3f\Big). \tag{56}$$

In the same way, we have for the first triadic terms:

$$III = \int \frac{\boldsymbol{rrr}}{r^6}\,\mathrm{d}t = \frac{1}{H}\int \frac{\hat{\boldsymbol{r}}\hat{\boldsymbol{r}}\hat{\boldsymbol{r}}}{r}\,\mathrm{d}f$$

$$= \frac{\mu}{H^3}\int (1 + e\cos f)\Big[\cos^3 f\,\hat{\boldsymbol{e}}\hat{\boldsymbol{e}}\hat{\boldsymbol{e}} + \cos^2 f\sin f(\hat{\boldsymbol{e}}\hat{\boldsymbol{e}}\hat{\boldsymbol{e}}_\perp + \hat{\boldsymbol{e}}\hat{\boldsymbol{e}}_\perp\hat{\boldsymbol{e}} + \hat{\boldsymbol{e}}_\perp\hat{\boldsymbol{e}}\hat{\boldsymbol{e}})$$

$$+ \cos f\sin^2 f(\hat{\boldsymbol{e}}\hat{\boldsymbol{e}}_\perp\hat{\boldsymbol{e}}_\perp + \hat{\boldsymbol{e}}_\perp\hat{\boldsymbol{e}}\hat{\boldsymbol{e}}_\perp + \hat{\boldsymbol{e}}_\perp\hat{\boldsymbol{e}}_\perp\hat{\boldsymbol{e}}) + \sin^3 f\,\hat{\boldsymbol{e}}_\perp\hat{\boldsymbol{e}}_\perp\hat{\boldsymbol{e}}_\perp\Big]\,\mathrm{d}f$$

$$= \frac{\mu}{H^3}\Big[III_{111}\hat{\boldsymbol{e}}\hat{\boldsymbol{e}}\hat{\boldsymbol{e}} + III_{112}(\hat{\boldsymbol{e}}\hat{\boldsymbol{e}}\hat{\boldsymbol{e}}_\perp + \hat{\boldsymbol{e}}\hat{\boldsymbol{e}}_\perp\hat{\boldsymbol{e}} + \hat{\boldsymbol{e}}_\perp\hat{\boldsymbol{e}}\hat{\boldsymbol{e}})$$

$$+ III_{122}(\hat{\boldsymbol{e}}\hat{\boldsymbol{e}}_\perp\hat{\boldsymbol{e}}_\perp + \hat{\boldsymbol{e}}_\perp\hat{\boldsymbol{e}}\hat{\boldsymbol{e}}_\perp + \hat{\boldsymbol{e}}_\perp\hat{\boldsymbol{e}}_\perp\hat{\boldsymbol{e}}) + III_{222}\hat{\boldsymbol{e}}_\perp\hat{\boldsymbol{e}}_\perp\hat{\boldsymbol{e}}_\perp\Big]. \tag{57}$$

Finally, for the last triadic term, we have

$$IV = \int \frac{\boldsymbol{rrr}}{r^7}\,\mathrm{d}t = \frac{1}{H}\int \frac{\hat{\boldsymbol{r}}\hat{\boldsymbol{r}}\hat{\boldsymbol{r}}}{r^2}\,\mathrm{d}f$$

$$= \frac{\mu^2}{H^5}\int (1 + e\cos f)^2\Big[\cos^3 f\,\hat{\boldsymbol{e}}\hat{\boldsymbol{e}}\hat{\boldsymbol{e}} + \cos^2 f\sin f(\hat{\boldsymbol{e}}\hat{\boldsymbol{e}}\hat{\boldsymbol{e}}_\perp + \hat{\boldsymbol{e}}\hat{\boldsymbol{e}}_\perp\hat{\boldsymbol{e}} + \hat{\boldsymbol{e}}_\perp\hat{\boldsymbol{e}}\hat{\boldsymbol{e}})$$

$$+ \cos f\sin^2 f(\hat{\boldsymbol{e}}\hat{\boldsymbol{e}}_\perp\hat{\boldsymbol{e}}_\perp + \hat{\boldsymbol{e}}_\perp\hat{\boldsymbol{e}}\hat{\boldsymbol{e}}_\perp + \hat{\boldsymbol{e}}_\perp\hat{\boldsymbol{e}}_\perp\hat{\boldsymbol{e}}) + \sin^3 f\,\hat{\boldsymbol{e}}_\perp\hat{\boldsymbol{e}}_\perp\hat{\boldsymbol{e}}_\perp\Big]\,\mathrm{d}f$$

$$= \frac{\mu^2}{H^5}\Big[IV_{111}\hat{\boldsymbol{e}}\hat{\boldsymbol{e}}\hat{\boldsymbol{e}} + IV_{112}(\hat{\boldsymbol{e}}\hat{\boldsymbol{e}}\hat{\boldsymbol{e}}_\perp + \hat{\boldsymbol{e}}\hat{\boldsymbol{e}}_\perp\hat{\boldsymbol{e}} + \hat{\boldsymbol{e}}_\perp\hat{\boldsymbol{e}}\hat{\boldsymbol{e}})$$

$$+ IV_{122}(\hat{\boldsymbol{e}}\hat{\boldsymbol{e}}_\perp\hat{\boldsymbol{e}}_\perp + \hat{\boldsymbol{e}}_\perp\hat{\boldsymbol{e}}\hat{\boldsymbol{e}}_\perp + \hat{\boldsymbol{e}}_\perp\hat{\boldsymbol{e}}_\perp\hat{\boldsymbol{e}}) + IV_{222}\hat{\boldsymbol{e}}_\perp\hat{\boldsymbol{e}}_\perp\hat{\boldsymbol{e}}_\perp\Big]. \tag{58}$$

where

$$I_0 = \int (1 + e\cos)\,\mathrm{d}f$$

$$= f + e\sin f, \tag{59a}$$

$$I_1 = \int (1 + e\cos f)^2\cos f\,\mathrm{d}f$$

$$= \frac{1}{12}\Big(12ef + (12 + 9e^2)\sin f + 6e\sin 2f + e^2\sin 3f\Big), \tag{59b}$$

18

$$I_2 = \int (1 + e \cos f)^2 \sin f \, \mathrm{d}f$$

$$= -\frac{1}{12} \Big((12 + 3e^2) \cos f + 6e \cos 2f + e^2 \cos 3f \Big), \tag{59c}$$

$$III_{111} = \int (1 + e \cos f) \cos^3 f \, \mathrm{d}f$$

$$= \frac{1}{96} \Big(36ef + 72 \sin f + 24e \sin 2f + 8 \sin 3f + 3e \sin 4f \Big), \tag{59d}$$

$$III_{112} = \int (1 + e \cos f) \cos^2 f \sin f \, \mathrm{d}f$$

$$= -\frac{1}{96} \Big(24 \cos f + 12e \cos 2f + 8 \cos 3f + 3e \cos 4f \Big), \tag{59e}$$

$$III_{122} = \int (1 + e \cos f) \cos f \sin^2 f \, \mathrm{d}f$$

$$= \frac{1}{96} \Big(12ef + 24 \sin f - 8 \sin 3f - 3e \sin 4f \Big), \tag{59f}$$

$$III_{222} = \int (1 + e \cos f) \sin^3 f \, \mathrm{d}f$$

$$= -\frac{1}{96} \Big(72 \cos f + 12e \cos 2f - 8 \cos 3f - 3e \cos 4f \Big), \tag{59g}$$

$$IV_{111} = \int (1 + e \cos f)^2 \cos^3 f \, \mathrm{d}f$$

$$= \frac{1}{240} \Big(180ef + 30(6 + 5e^2) \sin f + 120e \sin 2f + 5(4 + 5e^2) \sin 3f + 15e \sin 4f + 3e^2 \sin 5f \Big), \tag{59h}$$

$$IV_{112} = \int (1 + e \cos f)^2 \cos^2 f \sin f \, \mathrm{d}f$$

$$= -\frac{1}{240} \Big(30(2 + e^2) \cos f + 60e \cos 2f + 5(4 + 3e^2) \cos 3f + 15e \cos 4f + 3e^2 \cos 5f \Big), \tag{59i}$$

$$IV_{122} = \int (1 + e \cos f)^2 \cos f \sin^2 f \, \mathrm{d}f$$

$$= \frac{1}{240} \Big(60ef + 30(2 + e^2) \sin f - 5(4 + e^2) \sin 3f - 15e \sin 4f - 3e^2 \sin 5f \Big), \tag{59j}$$

$$IV_{222} = \int (1 + e \cos f)^2 \sin^3 f \, \mathrm{d}f$$

$$= -\frac{1}{240} \Big(30(6 + e^2) \cos f + 60e \cos 2f - 5(4 - e^2) \cos 3f - 15e \cos 4f - 3e^2 \cos 5f \Big). \tag{59k}$$

We also require the averages of these core integrals, which can easily be deduced by exploiting the Hansen coefficients (Eq. (38)) and equation of the center (Eq. (49)) expansions:

$$\overline{I}_0 = \frac{1}{2\pi} \int_0^{2\pi} (f + e \sin f) \, \mathrm{d}M$$

$$= \pi, \tag{60a}$$

$$\overline{I}_1 = \frac{1}{12} \frac{1}{2\pi} \int_0^{2\pi} \Big(12ef + (12 + 9e^2) \sin f + 6e \sin 2f + e^2 \sin 3f \Big) \, \mathrm{d}M$$

$$= \pi e, \tag{60b}$$

$$\overline{I}_2 = -\frac{1}{12} \frac{1}{2\pi} \int_0^{2\pi} \Big((12 + 3e^2) \cos f + 6e \cos 2f + e^2 \cos 3f \Big) \, \mathrm{d}M$$

$$= -\frac{1}{12} \Big((12 + 3e^2) X_0^{0,1} + 6e X_0^{0,2} + e^2 X_0^{0,3} \Big), \tag{60c}$$

$$\overline{II}_{11} = \frac{1}{12} \frac{1}{2\pi} \int_0^{2\pi} \Big(6f + 9e \sin f + 3 \sin 2f + e \sin 3f \Big) \, \mathrm{d}M$$

$$= \frac{1}{2}\pi, \tag{60d}$$

$$\overline{II}_{12} = -\frac{1}{12} \frac{1}{2\pi} \int_0^{2\pi} \Big(3e \cos f + 3 \cos 2f + e \cos 3f \Big) \, \mathrm{d}M$$

19

$$= -\frac{1}{12}\left(3eX_0^{0,1} + 3X_0^{0,2} + eX_0^{0,3}\right), \tag{60e}$$

$$\overline{II}_{22} = \frac{1}{12}\frac{1}{2\pi}\int_0^{2\pi}\left(6f + 3e\sin f - 3\sin 2f - e\sin 3f\right)\mathrm{d}M$$

$$= \frac{1}{2}\pi, \tag{60f}$$

$$\overline{III}_{111} = \frac{1}{96}\frac{1}{2\pi}\int_0^{2\pi}\left(36ef + 72\sin f + 24e\sin 2f + 8\sin 3f + 3e\sin 4f\right)\mathrm{d}M$$

$$= \frac{3}{8}\pi e, \tag{60g}$$

$$\overline{III}_{112} = -\frac{1}{96}\frac{1}{2\pi}\int_0^{2\pi}\left(24\cos f + 12e\cos 2f + 8\cos 3f + 3e\cos 4f\right)\mathrm{d}M$$

$$= -\frac{1}{96}\left(24X_0^{0,1} + 12eX_0^{0,2} + 8X_0^{0,3} + 3eX_0^{0,4}\right), \tag{60h}$$

$$\overline{III}_{122} = \frac{1}{96}\frac{1}{2\pi}\int_0^{2\pi}\left(12ef + 24\sin f - 8\sin 3f - 3e\sin 4f\right)\mathrm{d}M$$

$$= \frac{1}{8}\pi e, \tag{60i}$$

$$\overline{III}_{222} = -\frac{1}{96}\frac{1}{2\pi}\int_0^{2\pi}\left(72\cos f + 12e\cos 2f - 8\cos 3f - 3e\cos 4f\right)\mathrm{d}M$$

$$= -\frac{1}{96}\left(72X_0^{0,1} + 12eX_0^{0,2} - 8X_0^{0,3} - 3eX_0^{0,4}\right), \tag{60j}$$

$$\overline{IV}_{111} = \frac{1}{240}\frac{1}{2\pi}\int_0^{2\pi}\Big(180ef + 30(6 + 5e^2)\sin f + 120e\sin 2f$$
$$+ 5(4 + 5e^2)\sin 3f + 15e\sin 4f + 3e^2\sin 5f\Big)\mathrm{d}M$$

$$= \frac{3}{4}\pi e, \tag{60k}$$

$$\overline{IV}_{112} = -\frac{1}{240}\frac{1}{2\pi}\int_0^{2\pi}\Big(30(2 + e^2)\cos f + 60e\cos 2f$$
$$+ 5(4 + 3e^2)\cos 3f + 15e\cos 4f + 3e^2\cos 5f\Big)\mathrm{d}M$$

$$= -\frac{1}{240}\left(30(2 + e^2)X_0^{0,1} + 60eX_0^{0,2} + 5(4 + 3e^2)X_0^{0,3} + 15eX_0^{0,4} + 3e^2X_0^{0,5}\right), \tag{60l}$$

$$\overline{IV}_{122} = \frac{1}{240}\frac{1}{2\pi}\int_0^{2\pi}\Big(60ef + 30(2 + e^2)\sin f$$
$$- 5(4 + e^2)\sin 3f - 15e\sin 4f - 3e^2\sin 5f\Big)\mathrm{d}M$$

$$= \frac{1}{4}\pi e, \tag{60m}$$

$$\overline{IV}_{222} = -\frac{1}{240}\frac{1}{2\pi}\int_0^{2\pi}\Big(30(6 + e^2)\cos f + 60e\cos 2f$$
$$- 5(4 - e^2)\cos 3f - 15e\cos 4f - 3e^2\cos 5f\Big)\mathrm{d}M$$

$$= -\frac{1}{240}\left(30(6 + e^2)X_0^{0,1} + 60eX_0^{0,2} - 5(4 - e^2)X_0^{0,3} - 15eX_0^{0,4} - 3e^2X_0^{0,5}\right). \tag{60n}$$

The previous results are sufficient to derive the short-periodic perturbations in the eccentricity and angular momentum vectors, according to Eqs. (18a) and (18b), respectively. The mean longitude, however, requires the computation of additional integrals due to the mean motion Taylor-series terms, as detailed in Eqs. (22) and (23). These can be carried through to the core integrals, where again we can use Eqs. (38) and (49). In particular, using the mean anomaly as the dependent variable, we have

$$\widetilde{I}_1 = \frac{1}{12}\int\left(12ef + (12 + 9e^2)\sin f + 6e\sin 2f + e^2\sin 3f\right)\mathrm{d}M$$

$$= \frac{1}{12}\left[6eM^2 - \sum_{k=1}^{\infty}\frac{1}{k}\left(12e\phi_k + (12 + 9e^2)S_k^{0,1} + 6eS_k^{0,2} + e^2S_k^{0,3}\right)\cos kM\right], \tag{61a}$$

$$\widetilde{I}_2 = -\frac{1}{12}\int\Big((12+3e^2)\cos f + 6e\cos 2f + e^2\cos 3f\Big)\,\mathrm{d}M$$

$$= -\frac{1}{12}\Bigg[\Big((12+3e^2)C_0^{0,1} + 6eC_0^{0,2} + e^2C_0^{0,3}\Big)M$$

$$+ \sum_{k=1}^{\infty}\frac{1}{k}\Big((12+3e^2)C_k^{0,1} + 6eC_k^{0,2} + e^2C_k^{0,3}\Big)\sin kM\Bigg], \tag{61b}$$

$$\widetilde{II}_{11} = \frac{1}{12}\int\Big(6f + 9e\sin f + 3\sin 2f + e\sin 3f\Big)\,\mathrm{d}M$$

$$= \frac{1}{12}\Bigg[3M^2 - \sum_{k=1}^{\infty}\frac{1}{k}\Big(6\phi_k + 9eS_k^{0,1} + 3S_k^{0,2} + eS_k^{0,3}\Big)\cos kM\Bigg], \tag{61c}$$

$$\widetilde{II}_{12} = -\frac{1}{12}\int\Big(3e\cos f + 3\cos 2f + e\cos 3f\Big)\,\mathrm{d}M$$

$$= -\frac{1}{12}\Bigg[\Big(3eC_0^{0,1} + 3C_0^{0,2} + eC_0^{0,3}\Big)M$$

$$+ \sum_{k=1}^{\infty}\frac{1}{k}\Big(3eC_k^{0,1} + 3C_k^{0,2} + eC_k^{0,3}\Big)\sin kM\Bigg], \tag{61d}$$

$$\widetilde{II}_{22} = \frac{1}{12}\int\Big(6f + 3e\sin f - 3\sin 2f - e\sin 3f\Big)\,\mathrm{d}M$$

$$= \frac{1}{12}\Bigg[3M^2 - \sum_{k=1}^{\infty}\frac{1}{k}\Big(6\phi_k + 3eS_k^{0,1} - 3S_k^{0,2} - eS_k^{0,3}\Big)\cos kM\Bigg], \tag{61e}$$

$$\widetilde{III}_{111} = \frac{1}{96}\int\Big(36ef + 72\sin f + 24e\sin 2f + 8\sin 3f + 3e\sin 4f\Big)\,\mathrm{d}M$$

$$= \frac{1}{96}\Bigg[18eM^2 - \sum_{k=1}^{\infty}\frac{1}{k}\Big(36e\phi_k + 72S_k^{0,1} + 24eS_k^{0,2} + 8S_k^{0,3} + 3eS_k^{0,4}\Big)\cos kM\Bigg], \tag{61f}$$

$$\widetilde{III}_{112} = -\frac{1}{96}\int\Big(24\cos f + 12e\cos 2f + 8\cos 3f + 3e\cos 4f\Big)\,\mathrm{d}M$$

$$= -\frac{1}{96}\Bigg[\Big(24C_0^{0,1} + 12eC_0^{0,2} + 8C_0^{0,3} + 3eC_0^{0,4}\Big)M$$

$$+ \sum_{k=1}^{\infty}\frac{1}{k}\Big(24C_k^{0,1} + 12eC_k^{0,2} + 8C_k^{0,3} + 3eC_k^{0,4}\Big)\sin kM\Bigg], \tag{61g}$$

$$\widetilde{III}_{122} = \frac{1}{96}\int\Big(12ef + 24\sin f - 8\sin 3f - 3e\sin 4f\Big)\,\mathrm{d}M$$

$$= \frac{1}{96}\Bigg[6eM^2 - \sum_{k=1}^{\infty}\frac{1}{k}\Big(12e\phi_k + 24S_k^{0,1} - 8S_k^{0,3} - 3eS_k^{0,4}\Big)\cos kM\Bigg], \tag{61h}$$

$$\widetilde{III}_{222} = -\frac{1}{96}\int\Big(72\cos f + 12e\cos 2f - 8\cos 3f - 3e\cos 4f\Big)\,\mathrm{d}M$$

$$= -\frac{1}{96}\Bigg[\Big(72C_0^{0,1} + 12eC_0^{0,2} - 8C_0^{0,3} - 3eC_0^{0,4}\Big)M$$

$$+ \sum_{k=1}^{\infty}\frac{1}{k}\Big(72C_k^{0,1} + 12eC_k^{0,2} - 8C_k^{0,3} - 3eC_k^{0,4}\Big)\sin kM\Bigg], \tag{61i}$$

$$\widetilde{IV}_{111} = \frac{1}{240}\frac{1}{2\pi}\int_0^{2\pi}\Big(180ef + 30(6+5e^2)\sin f + 120e\sin 2f$$

$$+ 5(4+5e^2)\sin 3f + 15e\sin 4f + 3e^2\sin 5f\Big)\,\mathrm{d}M$$

$$= \frac{1}{240}\Bigg[90eM^2$$

$$-\sum_{k=1}^{\infty}\frac{1}{k}\Big(180e\phi_k+30(6+5e^2)S_k^{0,1}+120eS_k^{0,2}+5(4+5e^2)S_k^{0,3}+15eS_k^{0,4}+3e^2S_k^{0,5}\Big)\cos kM\Bigg],$$

(61j)

$$\widetilde{IV}_{112}=-\frac{1}{240}\int\Big(30(2+e^2)\cos f+60e\cos 2f$$

$$+5(4+3e^2)\cos 3f+15e\cos 4f+3e^2\cos 5f\Big)\,\mathrm{d}M$$

$$=-\frac{1}{240}\Bigg[\Big(30(2+e^2)C_0^{0,1}+60eC_0^{0,2}+5(4+3e^2)C_0^{0,3}+15eC_0^{0,4}+3e^2C_0^{0,5}\Big)M$$

$$+\sum_{k=1}^{\infty}\frac{1}{k}\Big(30(2+e^2)C_k^{0,1}+60eC_k^{0,2}+5(4+3e^2)C_k^{0,3}+15eC_k^{0,4}+3e^2C_k^{0,5}\Big)\sin kM\Bigg],$$

(61k)

$$\widetilde{IV}_{122}=\frac{1}{240}\int\Big(60ef+30(2+e^2)\sin f$$

$$-5(4+e^2)\sin 3f-15e\sin 4f-3e^2\sin 5f\Big)\,\mathrm{d}M$$

$$=\frac{1}{240}\Bigg[30eM^2$$

$$-\sum_{k=1}^{\infty}\frac{1}{k}\Big(60e\phi_k+30(2+e^2)S_k^{0,1}-5(4+e^2)S_k^{0,3}-15eS_k^{0,4}-3e^2S_k^{0,5}\Big)\cos kM\Bigg],$$

(61l)

$$\widetilde{IV}_{222}=-\frac{1}{240}\int\Big(30(6+e^2)\cos f+60e\cos 2f$$

$$-5(4-e^2)\cos 3f-15e\cos 4f-3e^2\cos 5f\Big)\,\mathrm{d}M$$

$$=-\frac{1}{240}\Bigg[\Big(30(6+e^2)C_0^{0,1}+60eC_0^{0,2}-5(4-e^2)C_0^{0,3}-15eC_0^{0,4}-3e^2C_0^{0,5}\Big)M$$

$$+\sum_{k=1}^{\infty}\frac{1}{k}\Big(30(6+e^2)C_k^{0,1}+60eC_k^{0,2}-5(4-e^2)C_k^{0,3}-15eC_k^{0,4}-3e^2C_k^{0,5}\Big)\sin kM\Bigg].$$

(61m)

Note that integrands are the same as those of the previous averages $\overline{I}_1$, $\overline{I}_2$, $\overline{II}_{11}$, …, in Eq. (60), but they differ in that the former are definite while the later are indefinite.

Finally, we require the averages of these doubly-integrated expressions:

$$\overline{\widetilde{I}}_1=\frac{2}{3}\pi^2 e,$$

(62a)

$$\overline{\widetilde{I}}_2=-\frac{1}{12}\Bigg[\Big((12+3e^2)C_0^{0,1}+6eC_0^{0,2}+e^2C_0^{0,3}\Big)\pi\Bigg],$$

(62b)

$$\overline{\widetilde{II}}_{11}=\frac{1}{3}\pi^2,$$

(62c)

$$\overline{\widetilde{II}}_{12}=-\frac{1}{12}\Bigg[\Big(3eC_0^{0,1}+3C_0^{0,2}+eC_0^{0,3}\Big)\pi\Bigg],$$

(62d)

$$\overline{\widetilde{II}}_{22}=\frac{1}{3}\pi^2,$$

(62e)

$$\overline{\widetilde{III}}_{111}=\frac{1}{4}\pi^2 e,$$

(62f)

$$\overline{\widetilde{III}}_{112}=-\frac{1}{96}\Bigg[\Big(24C_0^{0,1}+12eC_0^{0,2}+8C_0^{0,3}+3eC_0^{0,4}\Big)\pi\Bigg],$$

(62g)

$$\overline{\widetilde{III}}_{122}=\frac{1}{12}\pi^2 e,$$

(62h)

$$\overline{\widetilde{III}}_{222}=-\frac{1}{96}\Bigg[\Big(72C_0^{0,1}+12eC_0^{0,2}-8C_0^{0,3}-3eC_0^{0,4}\Big)\pi\Bigg],$$

(62i)

$$\overline{\widetilde{IV}}_{111} = \frac{1}{2}\pi^2 e, \tag{62j}$$

$$\overline{\widetilde{IV}}_{112} = -\frac{1}{240}\left[\left(30(2+e^2)C_0^{0,1} + 60eC_0^{0,2} + 5(4+3e^2)C_0^{0,3} + 15eC_0^{0,4} + 3e^2C_0^{0,5}\right)\pi\right], \tag{62k}$$

$$\overline{\widetilde{IV}}_{122} = \frac{1}{6}\pi^2 e, \tag{62l}$$

$$\overline{\widetilde{IV}}_{222} = -\frac{1}{240}\left[\left(30(6+e^2)C_0^{0,1} + 60eC_0^{0,2} - 5(4-e^2)C_0^{0,3} - 15eC_0^{0,4} - 3e^2C_0^{0,5}\right)\pi\right]. \tag{62m}$$

With these ingredients at hand, we now step through the derivation of the short-period corrections.

Eccentricity vector: Subtracting Eq. (30a) from Eq. (29a), holding the slowly varying orbital elements constant, and integrating, according to Eq. (17a), gives the short-periodic perturbations in $\boldsymbol{e}$ as

$$\begin{aligned}
\mathrm{d}\boldsymbol{e}^{sp}(t) = \frac{3J_2R^2}{2p^2}\Big\{ &I_1\left[\hat{\boldsymbol{e}}_\perp + 2(\hat{\boldsymbol{e}}\cdot\boldsymbol{p})\widetilde{\hat{\boldsymbol{h}}}\cdot\boldsymbol{p}\right] - I_2\left[\hat{\boldsymbol{e}} - 2(\hat{\boldsymbol{e}}_\perp\cdot\boldsymbol{p})\widetilde{\hat{\boldsymbol{h}}}\cdot\boldsymbol{p}\right] \\
&- 5IV_{111}(\hat{\boldsymbol{e}}\cdot\boldsymbol{p})^2\hat{\boldsymbol{e}}_\perp + 5IV_{112}\left[(\hat{\boldsymbol{e}}\cdot\boldsymbol{p})^2\hat{\boldsymbol{e}} - 2(\hat{\boldsymbol{e}}\cdot\boldsymbol{p})(\hat{\boldsymbol{e}}_\perp\cdot\boldsymbol{p})\hat{\boldsymbol{e}}_\perp\right] \\
&+ 5IV_{122}\left[2(\hat{\boldsymbol{e}}\cdot\boldsymbol{p})(\hat{\boldsymbol{e}}_\perp\cdot\boldsymbol{p})\hat{\boldsymbol{e}} - (\hat{\boldsymbol{e}}_\perp\cdot\boldsymbol{p})^2\hat{\boldsymbol{e}}_\perp\right] + 5IV_{222}(\hat{\boldsymbol{e}}_\perp\cdot\boldsymbol{p})^2\hat{\boldsymbol{e}} \\
&- 2eII_{11}(\hat{\boldsymbol{e}}\cdot\boldsymbol{p})(\hat{\boldsymbol{e}}_\perp\cdot\boldsymbol{p})\hat{\boldsymbol{e}} + 2eII_{12}\left[(\hat{\boldsymbol{e}}\cdot\boldsymbol{p})\boldsymbol{p} - (\hat{\boldsymbol{e}}\cdot\boldsymbol{p})(\hat{\boldsymbol{e}}_\perp\cdot\boldsymbol{p})\hat{\boldsymbol{e}}_\perp - (\hat{\boldsymbol{e}}_\perp\cdot\boldsymbol{p})^2\hat{\boldsymbol{e}}\right] \\
&+ 2eII_{22}\left[(\hat{\boldsymbol{e}}_\perp\cdot\boldsymbol{p})\boldsymbol{p} - (\hat{\boldsymbol{e}}_\perp\cdot\boldsymbol{p})^2\hat{\boldsymbol{e}}_\perp\right] + 2\left[(\hat{\boldsymbol{e}}\cdot\boldsymbol{p})^2 - (\hat{\boldsymbol{e}}_\perp\cdot\boldsymbol{p})^2\right](III_{112}\hat{\boldsymbol{e}} + III_{122}\hat{\boldsymbol{e}}_\perp) \\
&+ 2(\hat{\boldsymbol{e}}\cdot\boldsymbol{p})(\hat{\boldsymbol{e}}_\perp\cdot\boldsymbol{p})\left[(III_{122} - III_{111})\hat{\boldsymbol{e}} + (III_{222} - III_{112})\hat{\boldsymbol{e}}_\perp\right] \\
&+ \frac{1}{2}M\left[\left(1 - 5(\hat{\boldsymbol{h}}\cdot\boldsymbol{p})^2\right)\widetilde{\hat{\boldsymbol{h}}} + 2(\hat{\boldsymbol{h}}\cdot\boldsymbol{p})\widetilde{\boldsymbol{p}}\right]\cdot\boldsymbol{e}\Big\},
\end{aligned} \tag{63}$$

The mean value of this deviation with respect to the mean anomaly is given by

$$\begin{aligned}
\overline{\mathrm{d}\boldsymbol{e}}^{sp} = \frac{3J_2R^2}{2p^2}\Big\{ &\bar{I}_1\left[\hat{\boldsymbol{e}}_\perp + 2(\hat{\boldsymbol{e}}\cdot\boldsymbol{p})\widetilde{\hat{\boldsymbol{h}}}\cdot\boldsymbol{p}\right] - \bar{I}_2\left[\hat{\boldsymbol{e}} - 2(\hat{\boldsymbol{e}}_\perp\cdot\boldsymbol{p})\widetilde{\hat{\boldsymbol{h}}}\cdot\boldsymbol{p}\right] \\
&- 5\overline{IV}_{111}(\hat{\boldsymbol{e}}\cdot\boldsymbol{p})^2\hat{\boldsymbol{e}}_\perp + 5\overline{IV}_{112}\left[(\hat{\boldsymbol{e}}\cdot\boldsymbol{p})^2\hat{\boldsymbol{e}} - 2(\hat{\boldsymbol{e}}\cdot\boldsymbol{p})(\hat{\boldsymbol{e}}_\perp\cdot\boldsymbol{p})\hat{\boldsymbol{e}}_\perp\right] \\
&+ 5\overline{IV}_{122}\left[2(\hat{\boldsymbol{e}}\cdot\boldsymbol{p})(\hat{\boldsymbol{e}}_\perp\cdot\boldsymbol{p})\hat{\boldsymbol{e}} - (\hat{\boldsymbol{e}}_\perp\cdot\boldsymbol{p})^2\hat{\boldsymbol{e}}_\perp\right] + 5\overline{IV}_{222}(\hat{\boldsymbol{e}}_\perp\cdot\boldsymbol{p})^2\hat{\boldsymbol{e}} \\
&- 2e\overline{II}_{11}(\hat{\boldsymbol{e}}\cdot\boldsymbol{p})(\hat{\boldsymbol{e}}_\perp\cdot\boldsymbol{p})\hat{\boldsymbol{e}} + 2e\overline{II}_{12}\left[(\hat{\boldsymbol{e}}\cdot\boldsymbol{p})\boldsymbol{p} - (\hat{\boldsymbol{e}}\cdot\boldsymbol{p})(\hat{\boldsymbol{e}}_\perp\cdot\boldsymbol{p})\hat{\boldsymbol{e}}_\perp - (\hat{\boldsymbol{e}}_\perp\cdot\boldsymbol{p})^2\hat{\boldsymbol{e}}\right] \\
&+ 2e\overline{II}_{22}\left[(\hat{\boldsymbol{e}}_\perp\cdot\boldsymbol{p})\boldsymbol{p} - (\hat{\boldsymbol{e}}_\perp\cdot\boldsymbol{p})^2\hat{\boldsymbol{e}}_\perp\right] + 2\left[(\hat{\boldsymbol{e}}\cdot\boldsymbol{p})^2 - (\hat{\boldsymbol{e}}_\perp\cdot\boldsymbol{p})^2\right](\overline{III}_{112}\hat{\boldsymbol{e}} + \overline{III}_{122}\hat{\boldsymbol{e}}_\perp) \\
&+ 2(\hat{\boldsymbol{e}}\cdot\boldsymbol{p})(\hat{\boldsymbol{e}}_\perp\cdot\boldsymbol{p})\left[(\overline{III}_{122} - \overline{III}_{111})\hat{\boldsymbol{e}} + (\overline{III}_{222} - \overline{III}_{112})\hat{\boldsymbol{e}}_\perp\right] \\
&+ \frac{1}{2}\pi\left[\left(1 - 5(\hat{\boldsymbol{h}}\cdot\boldsymbol{p})^2\right)\widetilde{\hat{\boldsymbol{h}}} + 2(\hat{\boldsymbol{h}}\cdot\boldsymbol{p})\widetilde{\boldsymbol{p}}\right]\cdot\boldsymbol{e}\Big\},
\end{aligned} \tag{64}$$

We then have from Eq. (18a), after simplifying, that

$$\begin{aligned}
\boldsymbol{e}^{sp}(t) = \frac{3J_2R^2}{2p^2}\Big\{ &I_1\left[\hat{\boldsymbol{e}}_\perp + 2(\hat{\boldsymbol{e}}\cdot\boldsymbol{p})\widetilde{\hat{\boldsymbol{h}}}\cdot\boldsymbol{p}\right] - \hat{I}_2\left[\hat{\boldsymbol{e}} - 2(\hat{\boldsymbol{e}}_\perp\cdot\boldsymbol{p})\widetilde{\hat{\boldsymbol{h}}}\cdot\boldsymbol{p}\right] \\
&- 5IV_{111}(\hat{\boldsymbol{e}}\cdot\boldsymbol{p})^2\hat{\boldsymbol{e}}_\perp + 5\widehat{IV}_{112}\left[(\hat{\boldsymbol{e}}\cdot\boldsymbol{p})^2\hat{\boldsymbol{e}} - 2(\hat{\boldsymbol{e}}\cdot\boldsymbol{p})(\hat{\boldsymbol{e}}_\perp\cdot\boldsymbol{p})\hat{\boldsymbol{e}}_\perp\right] \\
&+ 5IV_{122}\left[2(\hat{\boldsymbol{e}}\cdot\boldsymbol{p})(\hat{\boldsymbol{e}}_\perp\cdot\boldsymbol{p})\hat{\boldsymbol{e}} - (\hat{\boldsymbol{e}}_\perp\cdot\boldsymbol{p})^2\hat{\boldsymbol{e}}_\perp\right] + 5\widehat{IV}_{222}(\hat{\boldsymbol{e}}_\perp\cdot\boldsymbol{p})^2\hat{\boldsymbol{e}} \\
&- 2eII_{11}(\hat{\boldsymbol{e}}\cdot\boldsymbol{p})(\hat{\boldsymbol{e}}_\perp\cdot\boldsymbol{p})\hat{\boldsymbol{e}} + 2e\widehat{II}_{12}\left[(\hat{\boldsymbol{e}}\cdot\boldsymbol{p})\boldsymbol{p} - (\hat{\boldsymbol{e}}\cdot\boldsymbol{p})(\hat{\boldsymbol{e}}_\perp\cdot\boldsymbol{p})\hat{\boldsymbol{e}}_\perp - (\hat{\boldsymbol{e}}_\perp\cdot\boldsymbol{p})^2\hat{\boldsymbol{e}}\right] \\
&+ 2eII_{22}\left[(\hat{\boldsymbol{e}}_\perp\cdot\boldsymbol{p})\boldsymbol{p} - (\hat{\boldsymbol{e}}_\perp\cdot\boldsymbol{p})^2\hat{\boldsymbol{e}}_\perp\right] + 2\left[(\hat{\boldsymbol{e}}\cdot\boldsymbol{p})^2 - (\hat{\boldsymbol{e}}_\perp\cdot\boldsymbol{p})^2\right]\left(\widehat{III}_{112}\hat{\boldsymbol{e}} + III_{122}\hat{\boldsymbol{e}}_\perp\right) \\
&+ 2(\hat{\boldsymbol{e}}\cdot\boldsymbol{p})(\hat{\boldsymbol{e}}_\perp\cdot\boldsymbol{p})(III_{122} - III_{111})\hat{\boldsymbol{e}} + 2(\hat{\boldsymbol{e}}\cdot\boldsymbol{p})(\hat{\boldsymbol{e}}_\perp\cdot\boldsymbol{p})\left(\widehat{III}_{222} - \widehat{III}_{112}\right)\hat{\boldsymbol{e}}_\perp \\
&+ \frac{1}{2}M\left[\left(1 - 5(\hat{\boldsymbol{h}}\cdot\boldsymbol{p})^2\right)\widetilde{\hat{\boldsymbol{h}}} + 2(\hat{\boldsymbol{h}}\cdot\boldsymbol{p})\widetilde{\boldsymbol{p}}\right]\cdot\boldsymbol{e}\Big\},
\end{aligned} \tag{65}$$

23

in which

$$\widehat{I}_2 = I_2 - \overline{I}_2, \tag{66a}$$

$$\widehat{II}_{12} = II_{12} - \overline{II}_{12}, \tag{66b}$$

$$\widehat{III}_{112} = III_{112} - \overline{III}_{112}, \tag{66c}$$

$$\widehat{III}_{222} = III_{222} - \overline{III}_{222}, \tag{66d}$$

$$\widehat{IV}_{112} = IV_{112} - \overline{IV}_{112}, \tag{66e}$$

$$\widehat{IV}_{222} = IV_{222} - \overline{IV}_{222}. \tag{66f}$$

Equation (65) can be cast into a simpler form that exposes the perifocal frame components, as given in Eq. (32a).

Angular momentum vector: In the same vein, following Eq. (17b), upon integrating, we have

$$\mathrm{d}\boldsymbol{H}^{sp}(t) = -\frac{3HJ_2R^2}{p^2}\hat{\boldsymbol{p}} \cdot \left[II_{11}\hat{\boldsymbol{e}}\hat{\boldsymbol{e}} + II_{12}(\hat{\boldsymbol{e}}\hat{\boldsymbol{e}}_\perp + \hat{\boldsymbol{e}}_\perp\hat{\boldsymbol{e}}) + II_{22}\hat{\boldsymbol{e}}_\perp\hat{\boldsymbol{e}}_\perp + \frac{1}{2}M\hat{\boldsymbol{h}}\hat{\boldsymbol{h}} \right] \cdot \widetilde{\hat{\boldsymbol{p}}}. \tag{67}$$

Computing the average gives

$$\overline{\mathrm{d}\boldsymbol{H}}^{sp} = -\frac{3HJ_2R^2}{p^2}\hat{\boldsymbol{p}} \cdot \left[\overline{II}_{11}\hat{\boldsymbol{e}}\hat{\boldsymbol{e}} + \overline{II}_{12}(\hat{\boldsymbol{e}}\hat{\boldsymbol{e}}_\perp + \hat{\boldsymbol{e}}_\perp\hat{\boldsymbol{e}}) + \overline{II}_{22}\hat{\boldsymbol{e}}_\perp\hat{\boldsymbol{e}}_\perp + \frac{1}{2}\pi\hat{\boldsymbol{h}}\hat{\boldsymbol{h}} \right] \cdot \widetilde{\hat{\boldsymbol{p}}}. \tag{68}$$

The result is then

$$\boldsymbol{H}^{sp}(t) = -\frac{3HJ_2R^2}{p^2}\hat{\boldsymbol{p}} \cdot \left[II_{11}\hat{\boldsymbol{e}}\hat{\boldsymbol{e}} + \widehat{II}_{12}(\hat{\boldsymbol{e}}\hat{\boldsymbol{e}}_\perp + \hat{\boldsymbol{e}}_\perp\hat{\boldsymbol{e}}) + II_{22}\hat{\boldsymbol{e}}_\perp\hat{\boldsymbol{e}}_\perp + \frac{1}{2}M\hat{\boldsymbol{h}}\hat{\boldsymbol{h}} \right] \cdot \widetilde{\hat{\boldsymbol{p}}}. \tag{69}$$

Equation (69) can also be written in a non-dyadic form as shown in Eq. (32b)

Mean longitude: We first note that

$$
\begin{aligned}
& \int \left[g_l(\overline{\boldsymbol{x}}, t) - \overline{g}_l(\overline{\boldsymbol{x}}) \right] \mathrm{d}t \\
&= \frac{3J_2R^2}{2p^2} \left\{ \frac{e}{1+\sqrt{1-e^2}} \left[I_1 - 3\left(IV_{111}(\hat{\boldsymbol{e}}\cdot\hat{\boldsymbol{p}})^2 + 2IV_{112}(\hat{\boldsymbol{e}}\cdot\hat{\boldsymbol{p}})(\hat{\boldsymbol{e}}_\perp\cdot\hat{\boldsymbol{p}}) + IV_{122}(\hat{\boldsymbol{e}}_\perp\cdot\hat{\boldsymbol{p}})^2 \right) \right. \right. \\
&\quad + 2\left(III_{222} - III_{112} + IV_{222} - IV_{112} \right)(\hat{\boldsymbol{e}}\cdot\hat{\boldsymbol{p}})(\hat{\boldsymbol{e}}_\perp\cdot\hat{\boldsymbol{p}}) \\
&\quad \left. + 2\left(III_{122} + IV_{122} \right)\left((\hat{\boldsymbol{e}}\cdot\hat{\boldsymbol{p}})^2 - (\hat{\boldsymbol{e}}_\perp\cdot\hat{\boldsymbol{p}})^2 \right) \right] \\
&\quad - 2\left(3\sqrt{1-e^2} + \frac{\hat{\boldsymbol{h}}\cdot\hat{\boldsymbol{p}}}{1+\hat{\boldsymbol{h}}\cdot\hat{\boldsymbol{p}}} \right)\left(II_{11}(\hat{\boldsymbol{e}}\cdot\hat{\boldsymbol{p}})^2 + 2II_{12}(\hat{\boldsymbol{e}}\cdot\hat{\boldsymbol{p}})(\hat{\boldsymbol{e}}_\perp\cdot\hat{\boldsymbol{p}}) + II_{22}(\hat{\boldsymbol{e}}_\perp\cdot\hat{\boldsymbol{p}})^2 \right) \\
&\quad \left. + 2\sqrt{1-e^2}I_0 - \frac{1}{2}M\left[\sqrt{1-e^2}\left(3(\hat{\boldsymbol{h}}\cdot\hat{\boldsymbol{p}})^2 - 1 \right) + 5(\hat{\boldsymbol{h}}\cdot\hat{\boldsymbol{p}})^2 - 2(\hat{\boldsymbol{h}}\cdot\hat{\boldsymbol{p}}) - 1 \right] \right\},
\end{aligned}
\tag{70}
$$

and

$$
\begin{aligned}
& \frac{1}{T}\int_0^T \int \left[g_l(\overline{\boldsymbol{x}}, t) - \overline{g}_l(\overline{\boldsymbol{x}}) \right] \mathrm{d}t^2 \\
&= \frac{3J_2R^2}{2p^2} \left\{ \frac{e}{1+\sqrt{1-e^2}} \left[\overline{I}_1 - 3\left(\overline{IV}_{111}(\hat{\boldsymbol{e}}\cdot\hat{\boldsymbol{p}})^2 + 2\overline{IV}_{112}(\hat{\boldsymbol{e}}\cdot\hat{\boldsymbol{p}})(\hat{\boldsymbol{e}}_\perp\cdot\hat{\boldsymbol{p}}) + \overline{IV}_{122}(\hat{\boldsymbol{e}}_\perp\cdot\hat{\boldsymbol{p}})^2 \right) \right. \right. \\
&\quad + 2\left(\overline{III}_{222} - \overline{III}_{112} + \overline{IV}_{222} - \overline{IV}_{112} \right)(\hat{\boldsymbol{e}}\cdot\hat{\boldsymbol{p}})(\hat{\boldsymbol{e}}_\perp\cdot\hat{\boldsymbol{p}}) \\
&\quad \left. + 2\left(\overline{III}_{122} + \overline{IV}_{122} \right)\left((\hat{\boldsymbol{e}}\cdot\hat{\boldsymbol{p}})^2 - (\hat{\boldsymbol{e}}_\perp\cdot\hat{\boldsymbol{p}})^2 \right) \right] \\
&\quad - 2\left(3\sqrt{1-e^2} + \frac{\hat{\boldsymbol{h}}\cdot\hat{\boldsymbol{p}}}{1+\hat{\boldsymbol{h}}\cdot\hat{\boldsymbol{p}}} \right)\left(\overline{II}_{11}(\hat{\boldsymbol{e}}\cdot\hat{\boldsymbol{p}})^2 + 2\overline{II}_{12}(\hat{\boldsymbol{e}}\cdot\hat{\boldsymbol{p}})(\hat{\boldsymbol{e}}_\perp\cdot\hat{\boldsymbol{p}}) + \overline{II}_{22}(\hat{\boldsymbol{e}}_\perp\cdot\hat{\boldsymbol{p}})^2 \right) \\
&\quad \left. + 2\sqrt{1-e^2}\overline{I}_0 - \frac{1}{2}\pi\left[\sqrt{1-e^2}\left(3(\hat{\boldsymbol{h}}\cdot\hat{\boldsymbol{p}})^2 - 1 \right) + 5(\hat{\boldsymbol{h}}\cdot\hat{\boldsymbol{p}})^2 - 2(\hat{\boldsymbol{h}}\cdot\hat{\boldsymbol{p}}) - 1 \right] \right\}.
\end{aligned}
\tag{71}
$$

Furthermore,

$$\int \boldsymbol{e}^{sp}(\tau)\,\mathrm{d}\tau$$

$$= \frac{3J_2R^2}{2np^2}\Bigg\{\widetilde{I}_1\left[\hat{\boldsymbol{e}}_\perp + 2(\hat{\boldsymbol{e}}\cdot\hat{\boldsymbol{p}})\widetilde{\hat{\boldsymbol{h}}}\cdot\hat{\boldsymbol{p}}\right] - (\widetilde{I}_2 - \bar{I}_2 M)\left[\hat{\boldsymbol{e}} - 2(\hat{\boldsymbol{e}}_\perp\cdot\hat{\boldsymbol{p}})\widetilde{\hat{\boldsymbol{h}}}\cdot\hat{\boldsymbol{p}}\right]$$

$$- 5\widetilde{IV}_{111}(\hat{\boldsymbol{e}}\cdot\hat{\boldsymbol{p}})^2\hat{\boldsymbol{e}}_\perp + 5(\widetilde{IV}_{112} - \overline{IV}_{112}M)\left[(\hat{\boldsymbol{e}}\cdot\hat{\boldsymbol{p}})^2\hat{\boldsymbol{e}} - 2(\hat{\boldsymbol{e}}\cdot\hat{\boldsymbol{p}})(\hat{\boldsymbol{e}}_\perp\cdot\hat{\boldsymbol{p}})\hat{\boldsymbol{e}}_\perp\right]$$

$$+ 5\widetilde{IV}_{122}\left[2(\hat{\boldsymbol{e}}\cdot\hat{\boldsymbol{p}})(\hat{\boldsymbol{e}}_\perp\cdot\hat{\boldsymbol{p}})\hat{\boldsymbol{e}} - (\hat{\boldsymbol{e}}_\perp\cdot\hat{\boldsymbol{p}})^2\hat{\boldsymbol{e}}_\perp\right] + 5(\widetilde{IV}_{222} - \overline{IV}_{222}M)(\hat{\boldsymbol{e}}_\perp\cdot\hat{\boldsymbol{p}})^2\hat{\boldsymbol{e}}$$

$$- 2e\widetilde{II}_{11}(\hat{\boldsymbol{e}}\cdot\hat{\boldsymbol{p}})(\hat{\boldsymbol{e}}_\perp\cdot\hat{\boldsymbol{p}})\hat{\boldsymbol{e}} + 2e(\widetilde{II}_{12} - \overline{II}_{12}M)\left[(\hat{\boldsymbol{e}}\cdot\hat{\boldsymbol{p}})\hat{\boldsymbol{p}} - (\hat{\boldsymbol{e}}\cdot\hat{\boldsymbol{p}})(\hat{\boldsymbol{e}}_\perp\cdot\hat{\boldsymbol{p}})\hat{\boldsymbol{e}}_\perp - (\hat{\boldsymbol{e}}_\perp\cdot\hat{\boldsymbol{p}})^2\hat{\boldsymbol{e}}\right]$$

$$+ 2e\widetilde{II}_{22}\left[(\hat{\boldsymbol{e}}_\perp\cdot\hat{\boldsymbol{p}})\hat{\boldsymbol{p}} - (\hat{\boldsymbol{e}}_\perp\cdot\hat{\boldsymbol{p}})^2\hat{\boldsymbol{e}}_\perp\right] + 2\left[(\hat{\boldsymbol{e}}\cdot\hat{\boldsymbol{p}})^2 - (\hat{\boldsymbol{e}}_\perp\cdot\hat{\boldsymbol{p}})^2\right]\left((\widetilde{III}_{112} - \overline{III}_{112}M)\hat{\boldsymbol{e}} + \widetilde{III}_{122}\hat{\boldsymbol{e}}_\perp\right)$$

$$+ 2(\hat{\boldsymbol{e}}\cdot\hat{\boldsymbol{p}})(\hat{\boldsymbol{e}}_\perp\cdot\hat{\boldsymbol{p}})\left[\left(\widetilde{III}_{122} - \widetilde{III}_{111}\right)\hat{\boldsymbol{e}} + \left(\widetilde{III}_{222} - \overline{III}_{222}M - \widetilde{III}_{112} + \overline{III}_{112}M\right)\hat{\boldsymbol{e}}_\perp\right]$$

$$+ \frac{1}{4}M^2\left[\left(1 - 5(\hat{\boldsymbol{h}}\cdot\hat{\boldsymbol{p}})^2\right)\widetilde{\hat{\boldsymbol{h}}} + 2(\hat{\boldsymbol{h}}\cdot\hat{\boldsymbol{p}})\widetilde{\hat{\boldsymbol{p}}}\right]\cdot\boldsymbol{e}\Bigg\}, \tag{72}$$

$$\int \boldsymbol{H}^{sp}(t)\,\mathrm{d}t$$

$$= -\frac{3HJ_2R^2}{np^2}\hat{\boldsymbol{p}}\cdot\left[\widetilde{II}_{11}\hat{\boldsymbol{e}}\hat{\boldsymbol{e}} + (\widetilde{II}_{12} - \overline{II}_{12}M)(\hat{\boldsymbol{e}}\hat{\boldsymbol{e}}_\perp + \hat{\boldsymbol{e}}_\perp\hat{\boldsymbol{e}}) + \widetilde{II}_{22}\hat{\boldsymbol{e}}_\perp\hat{\boldsymbol{e}}_\perp + \frac{1}{4}M^2\hat{\boldsymbol{h}}\hat{\boldsymbol{h}}\right]\cdot\widetilde{\hat{\boldsymbol{p}}}, \tag{73}$$

We also have that

$$\frac{1}{T}\int_0^T\int \boldsymbol{e}^{sp}(t)\,\mathrm{d}t^2$$

$$= \frac{3J_2R^2}{2np^2}\Bigg\{\widetilde{\widetilde{I}}_1\left[\hat{\boldsymbol{e}}_\perp + 2(\hat{\boldsymbol{e}}\cdot\hat{\boldsymbol{p}})\widetilde{\hat{\boldsymbol{h}}}\cdot\hat{\boldsymbol{p}}\right] - (\widetilde{\widetilde{I}}_2 - \bar{I}_2\pi)\left[\hat{\boldsymbol{e}} - 2(\hat{\boldsymbol{e}}_\perp\cdot\hat{\boldsymbol{p}})\widetilde{\hat{\boldsymbol{h}}}\cdot\hat{\boldsymbol{p}}\right]$$

$$- 5\widetilde{\widetilde{IV}}_{111}(\hat{\boldsymbol{e}}\cdot\hat{\boldsymbol{p}})^2\hat{\boldsymbol{e}}_\perp + 5(\widetilde{\widetilde{IV}}_{112} - \overline{IV}_{112}\pi)\left[(\hat{\boldsymbol{e}}\cdot\hat{\boldsymbol{p}})^2\hat{\boldsymbol{e}} - 2(\hat{\boldsymbol{e}}\cdot\hat{\boldsymbol{p}})(\hat{\boldsymbol{e}}_\perp\cdot\hat{\boldsymbol{p}})\hat{\boldsymbol{e}}_\perp\right]$$

$$+ 5\widetilde{\widetilde{IV}}_{122}\left[2(\hat{\boldsymbol{e}}\cdot\hat{\boldsymbol{p}})(\hat{\boldsymbol{e}}_\perp\cdot\hat{\boldsymbol{p}})\hat{\boldsymbol{e}} - (\hat{\boldsymbol{e}}_\perp\cdot\hat{\boldsymbol{p}})^2\hat{\boldsymbol{e}}_\perp\right] + 5(\widetilde{\widetilde{IV}}_{222} - \overline{IV}_{222}\pi)(\hat{\boldsymbol{e}}_\perp\cdot\hat{\boldsymbol{p}})^2\hat{\boldsymbol{e}}$$

$$- 2e\widetilde{\widetilde{II}}_{11}(\hat{\boldsymbol{e}}\cdot\hat{\boldsymbol{p}})(\hat{\boldsymbol{e}}_\perp\cdot\hat{\boldsymbol{p}})\hat{\boldsymbol{e}} + 2e(\widetilde{\widetilde{II}}_{12} - \overline{II}_{12}\pi)\left[(\hat{\boldsymbol{e}}\cdot\hat{\boldsymbol{p}})\hat{\boldsymbol{p}} - (\hat{\boldsymbol{e}}\cdot\hat{\boldsymbol{p}})(\hat{\boldsymbol{e}}_\perp\cdot\hat{\boldsymbol{p}})\hat{\boldsymbol{e}}_\perp - (\hat{\boldsymbol{e}}_\perp\cdot\hat{\boldsymbol{p}})^2\hat{\boldsymbol{e}}\right]$$

$$+ 2e\widetilde{\widetilde{II}}_{22}\left[(\hat{\boldsymbol{e}}_\perp\cdot\hat{\boldsymbol{p}})\hat{\boldsymbol{p}} - (\hat{\boldsymbol{e}}_\perp\cdot\hat{\boldsymbol{p}})^2\hat{\boldsymbol{e}}_\perp\right] + 2\left[(\hat{\boldsymbol{e}}\cdot\hat{\boldsymbol{p}})^2 - (\hat{\boldsymbol{e}}_\perp\cdot\hat{\boldsymbol{p}})^2\right]\left((\widetilde{\widetilde{III}}_{112} - \overline{III}_{112}\pi)\hat{\boldsymbol{e}} + \widetilde{\widetilde{III}}_{122}\hat{\boldsymbol{e}}_\perp\right)$$

$$+ 2(\hat{\boldsymbol{e}}\cdot\hat{\boldsymbol{p}})(\hat{\boldsymbol{e}}_\perp\cdot\hat{\boldsymbol{p}})\left[\left(\widetilde{\widetilde{III}}_{122} - \widetilde{\widetilde{III}}_{111}\right)\hat{\boldsymbol{e}} + \left(\widetilde{\widetilde{III}}_{222} - \overline{III}_{222}\pi - \widetilde{\widetilde{III}}_{112} + \overline{III}_{112}\pi\right)\hat{\boldsymbol{e}}_\perp\right]$$

$$+ \frac{1}{3}\pi^2\left[\left(1 - 5(\hat{\boldsymbol{h}}\cdot\hat{\boldsymbol{p}})^2\right)\widetilde{\hat{\boldsymbol{h}}} + 2(\hat{\boldsymbol{h}}\cdot\hat{\boldsymbol{p}})\widetilde{\hat{\boldsymbol{p}}}\right]\cdot\boldsymbol{e}\Bigg\}, \tag{74}$$

$$\frac{1}{T}\int_0^T\int \boldsymbol{H}^{sp}(t)\,\mathrm{d}t^2$$

$$= -\frac{3HJ_2R^2}{np^2}\hat{\boldsymbol{p}}\cdot\left[\widetilde{\widetilde{II}}_{11}\hat{\boldsymbol{e}}\hat{\boldsymbol{e}} + (\widetilde{\widetilde{II}}_{12} - \overline{II}_{12}\pi)(\hat{\boldsymbol{e}}\hat{\boldsymbol{e}}_\perp + \hat{\boldsymbol{e}}_\perp\hat{\boldsymbol{e}}) + \widetilde{\widetilde{II}}_{22}\hat{\boldsymbol{e}}_\perp\hat{\boldsymbol{e}}_\perp + \frac{1}{3}\pi^2\hat{\boldsymbol{h}}\hat{\boldsymbol{h}}\right]\cdot\widetilde{\hat{\boldsymbol{p}}}, \tag{75}$$

The short-periodic perturbations for mean longitude can thus be stated as

$$l^{sp}(t) = \mathrm{d}l^{sp}(t) - \overline{\mathrm{d}l}^{sp}(t)$$

$$= \frac{3J_2R^2}{2p^2}\Bigg\{\frac{e}{1+\sqrt{1-e^2}}\Big[(I_1 - \bar{I}_1) - 3\Big((IV_{111} - \overline{IV}_{111})(\hat{\boldsymbol{e}}\cdot\hat{\boldsymbol{p}})^2$$

$$+ 2(IV_{112} - \overline{IV}_{112})(\hat{\boldsymbol{e}}\cdot\hat{\boldsymbol{p}})(\hat{\boldsymbol{e}}_\perp\cdot\hat{\boldsymbol{p}}) + (IV_{122} - \overline{IV}_{122})(\hat{\boldsymbol{e}}_\perp\cdot\hat{\boldsymbol{p}})^2\Big)$$

$$+ 2\left(III_{222} - \overline{III}_{222} - III_{112} + \overline{III}_{112} + IV_{222} - \overline{IV}_{222} - IV_{112} + \overline{IV}_{112}\right)(\hat{\boldsymbol{e}}\cdot\hat{\boldsymbol{p}})(\hat{\boldsymbol{e}}_\perp\cdot\hat{\boldsymbol{p}})$$

$$+ 2\left(III_{122} - \overline{III}_{122} + IV_{122} - \overline{IV}_{122}\right)\left((\hat{\boldsymbol{e}}\cdot\hat{\boldsymbol{p}})^2 - (\hat{\boldsymbol{e}}_\perp\cdot\hat{\boldsymbol{p}})^2\right)\Big]$$

$$- 2\left(3\sqrt{1-e^2} + \frac{\hat{\boldsymbol{h}}\cdot\hat{\boldsymbol{p}}}{1+\hat{\boldsymbol{h}}\cdot\hat{\boldsymbol{p}}}\right)\left((II_{11} - \overline{II}_{11})(\hat{\boldsymbol{e}}\cdot\hat{\boldsymbol{p}})^2\right.$$

$$+ 2(II_{12} - \overline{II}_{12})(\hat{\boldsymbol{e}} \cdot \hat{\boldsymbol{p}})(\hat{\boldsymbol{e}}_\perp \cdot \hat{\boldsymbol{p}}) + (II_{22} - \overline{II}_{22})(\hat{\boldsymbol{e}}_\perp \cdot \hat{\boldsymbol{p}})^2\Big)$$

$$+ 2\sqrt{1-e^2}(I_0 - \overline{I}_0) - \frac{1}{2}(M - \pi)\left[\sqrt{1-e^2}\left(3(\hat{\boldsymbol{h}} \cdot \hat{\boldsymbol{p}})^2 - 1\right) + 5(\hat{\boldsymbol{h}} \cdot \hat{\boldsymbol{p}})^2 - 2(\hat{\boldsymbol{h}} \cdot \hat{\boldsymbol{p}}) - 1\right]\Bigg\}$$

$$- \frac{3J_2 R^2}{2np^2}\frac{3\mu^2}{H^3}\sqrt{1-e^2}\Bigg\{(\widetilde{I}_1 - \widetilde{\overline{I}}_1)\left[\hat{\boldsymbol{e}}_\perp + 2(\hat{\boldsymbol{e}} \cdot \hat{\boldsymbol{p}})\widetilde{\hat{\boldsymbol{h}}} \cdot \hat{\boldsymbol{p}}\right] - (\widetilde{I}_2 - \widetilde{\overline{I}}_2 - \overline{I}_2(M - \pi))\left[\hat{\boldsymbol{e}} - 2(\hat{\boldsymbol{e}}_\perp \cdot \hat{\boldsymbol{p}})\widetilde{\hat{\boldsymbol{h}}} \cdot \hat{\boldsymbol{p}}\right]$$

$$- 5(\widetilde{IV}_{111} - \widetilde{\overline{IV}}_{111})(\hat{\boldsymbol{e}} \cdot \hat{\boldsymbol{p}})^2\hat{\boldsymbol{e}}_\perp + 5(\widetilde{IV}_{112} - \widetilde{\overline{IV}}_{112} - \overline{IV}_{112}(M - \pi))\left[(\hat{\boldsymbol{e}} \cdot \hat{\boldsymbol{p}})^2\hat{\boldsymbol{e}} - 2(\hat{\boldsymbol{e}} \cdot \hat{\boldsymbol{p}})(\hat{\boldsymbol{e}}_\perp \cdot \hat{\boldsymbol{p}})\hat{\boldsymbol{e}}_\perp\right]$$

$$+ 5(\widetilde{IV}_{122} - \widetilde{\overline{IV}}_{122})\left[2(\hat{\boldsymbol{e}} \cdot \hat{\boldsymbol{p}})(\hat{\boldsymbol{e}}_\perp \cdot \hat{\boldsymbol{p}})\hat{\boldsymbol{e}} - (\hat{\boldsymbol{e}}_\perp \cdot \hat{\boldsymbol{p}})^2\hat{\boldsymbol{e}}_\perp\right] + 5(\widetilde{IV}_{222} - \widetilde{\overline{IV}}_{222} - \overline{IV}_{222}(M - \pi))(\hat{\boldsymbol{e}}_\perp \cdot \hat{\boldsymbol{p}})^2\hat{\boldsymbol{e}}$$

$$- 2e(\widetilde{II}_{11} - \widetilde{\overline{II}}_{11})(\hat{\boldsymbol{e}} \cdot \hat{\boldsymbol{p}})(\hat{\boldsymbol{e}}_\perp \cdot \hat{\boldsymbol{p}})\hat{\boldsymbol{e}} + 2e(\widetilde{II}_{12} - \widetilde{\overline{II}}_{12} - \overline{II}_{12}(M - \pi))\left[(\hat{\boldsymbol{e}} \cdot \hat{\boldsymbol{p}})\hat{\boldsymbol{p}} - (\hat{\boldsymbol{e}} \cdot \hat{\boldsymbol{p}})(\hat{\boldsymbol{e}}_\perp \cdot \hat{\boldsymbol{p}})\hat{\boldsymbol{e}}_\perp - (\hat{\boldsymbol{e}}_\perp \cdot \hat{\boldsymbol{p}})^2\hat{\boldsymbol{e}}\right]$$

$$+ 2e(\widetilde{II}_{22} - \widetilde{\overline{II}}_{22})\left[(\hat{\boldsymbol{e}}_\perp \cdot \hat{\boldsymbol{p}})\hat{\boldsymbol{p}} - (\hat{\boldsymbol{e}}_\perp \cdot \hat{\boldsymbol{p}})^2\hat{\boldsymbol{e}}_\perp\right]$$

$$+ 2\left[(\hat{\boldsymbol{e}} \cdot \hat{\boldsymbol{p}})^2 - (\hat{\boldsymbol{e}}_\perp \cdot \hat{\boldsymbol{p}})^2\right]\left((\widetilde{III}_{112} - \widetilde{\overline{III}}_{112} - \overline{III}_{112}(M - \pi))\hat{\boldsymbol{e}} + (\widetilde{III}_{122} - \widetilde{\overline{III}}_{122})\hat{\boldsymbol{e}}_\perp\right)$$

$$+ 2(\hat{\boldsymbol{e}} \cdot \hat{\boldsymbol{p}})(\hat{\boldsymbol{e}}_\perp \cdot \hat{\boldsymbol{p}})\Big[\left(\widetilde{III}_{122} - \widetilde{\overline{III}}_{122} - \widetilde{III}_{111} + \widetilde{\overline{III}}_{111}\right)\hat{\boldsymbol{e}}$$

$$+ \left(\widetilde{III}_{222} - \widetilde{\overline{III}}_{222} - \overline{III}_{222}(M - \pi) - \widetilde{III}_{112} + \widetilde{\overline{III}}_{112} + \overline{III}_{112}(M - \pi)\right)\hat{\boldsymbol{e}}_\perp\Big]$$

$$+ \frac{1}{12}(3M^2 - 4\pi^2)\left[\left(1 - 5(\hat{\boldsymbol{h}} \cdot \hat{\boldsymbol{p}})^2\right)\hat{\boldsymbol{h}} + 2(\hat{\boldsymbol{h}} \cdot \hat{\boldsymbol{p}})\hat{\boldsymbol{p}}\right] \cdot \widetilde{\boldsymbol{e}}\Bigg\} \cdot \boldsymbol{e}$$

$$+ \frac{3HJ_2 R^2}{np^2}\frac{3\mu^2}{H^5}(1-e^2)^{3/2}\Bigg\{\hat{\boldsymbol{p}} \cdot \left[(\widetilde{II}_{11} - \widetilde{\overline{II}}_{11})\hat{\boldsymbol{e}}\hat{\boldsymbol{e}} + (\widetilde{II}_{12} - \widetilde{\overline{II}}_{12} - \overline{II}_{12}(M - \pi))(\hat{\boldsymbol{e}}\hat{\boldsymbol{e}}_\perp + \hat{\boldsymbol{e}}_\perp\hat{\boldsymbol{e}})\right.$$

$$+ (\widetilde{II}_{22} - \widetilde{\overline{II}}_{22})\hat{\boldsymbol{e}}_\perp\hat{\boldsymbol{e}}_\perp + \frac{1}{12}(3M^2 - 4\pi^2)\hat{\boldsymbol{h}}\hat{\boldsymbol{h}}\Big] \cdot \widetilde{\boldsymbol{p}}\Bigg\} \cdot \boldsymbol{H}. \tag{76}$$

Simplifying gives

$$l^{sp}(t) = \frac{3J_2 R^2}{2p^2}\Bigg\{\frac{e}{1 + \sqrt{1-e^2}}\Big[I_1 - 3\Big(IV_{111}(\hat{\boldsymbol{e}} \cdot \hat{\boldsymbol{p}})^2 + 2\widehat{IV}_{112}(\hat{\boldsymbol{e}} \cdot \hat{\boldsymbol{p}})(\hat{\boldsymbol{e}}_\perp \cdot \hat{\boldsymbol{p}}) + IV_{122}(\hat{\boldsymbol{e}}_\perp \cdot \hat{\boldsymbol{p}})^2\Big)$$

$$+ 2\left(\widehat{III}_{222} - \widehat{III}_{112} + \widehat{IV}_{222} - \widehat{IV}_{112}\right)(\hat{\boldsymbol{e}} \cdot \hat{\boldsymbol{p}})(\hat{\boldsymbol{e}}_\perp \cdot \hat{\boldsymbol{p}}) + 2\left(III_{122} + IV_{122}\right)\left((\hat{\boldsymbol{e}} \cdot \hat{\boldsymbol{p}})^2 - (\hat{\boldsymbol{e}}_\perp \cdot \hat{\boldsymbol{p}})^2\right)\Big]$$

$$- 2\left(3\sqrt{1-e^2} + \frac{\hat{\boldsymbol{h}} \cdot \hat{\boldsymbol{p}}}{1 + \hat{\boldsymbol{h}} \cdot \hat{\boldsymbol{p}}}\right)\left(II_{11}(\hat{\boldsymbol{e}} \cdot \hat{\boldsymbol{p}})^2 + 2\widehat{II}_{12}(\hat{\boldsymbol{e}} \cdot \hat{\boldsymbol{p}})(\hat{\boldsymbol{e}}_\perp \cdot \hat{\boldsymbol{p}}) + II_{22}(\hat{\boldsymbol{e}}_\perp \cdot \hat{\boldsymbol{p}})^2\right) + 2\sqrt{1-e^2}I_0$$

$$- \frac{1}{2}M\left[\sqrt{1-e^2}\left(3(\hat{\boldsymbol{h}} \cdot \hat{\boldsymbol{p}})^2 - 1\right) + 5(\hat{\boldsymbol{h}} \cdot \hat{\boldsymbol{p}})^2 - 2(\hat{\boldsymbol{h}} \cdot \hat{\boldsymbol{p}}) - 1\right]$$

$$+ \frac{3eH}{np^2}\sqrt{1-e^2}\Big[2\left(\widetilde{\mathcal{IV}} + e\widetilde{\mathcal{II}}\right)(\hat{\boldsymbol{e}} \cdot \hat{\boldsymbol{p}})(\hat{\boldsymbol{e}}_\perp \cdot \hat{\boldsymbol{p}}) + \widehat{\overline{I}}_2\left(1 + 2(\hat{\boldsymbol{e}}_\perp \cdot \hat{\boldsymbol{p}})^2\right)$$

$$- 5\widehat{\widetilde{IV}}_{112}(\hat{\boldsymbol{e}} \cdot \hat{\boldsymbol{p}})^2 - 5\widehat{\widetilde{IV}}_{222}(\hat{\boldsymbol{e}}_\perp \cdot \hat{\boldsymbol{p}})^2 - 2\left(\widehat{\widetilde{III}}_{112} + e\widehat{\widetilde{II}}_{12}\right)\left((\hat{\boldsymbol{e}} \cdot \hat{\boldsymbol{p}})^2 - (\hat{\boldsymbol{e}}_\perp \cdot \hat{\boldsymbol{p}})^2\right)\Big]$$

$$+ \frac{6H}{np^2}(1-e^2)^{3/2}\Big[\widetilde{\mathcal{II}}(\hat{\boldsymbol{e}} \cdot \hat{\boldsymbol{p}})(\hat{\boldsymbol{e}}_\perp \cdot \hat{\boldsymbol{p}}) - \widehat{\widetilde{II}}_{12}\left((\hat{\boldsymbol{e}} \cdot \hat{\boldsymbol{p}})^2 - (\hat{\boldsymbol{e}}_\perp \cdot \hat{\boldsymbol{p}})^2\right)\Big]\Bigg\}, \tag{77}$$

where

$$\widehat{\widetilde{I}}_2 = \widetilde{I}_2 - \widetilde{\overline{I}}_2 - \overline{I}_2(M - \pi)$$

$$= -\frac{1}{12}\sum_{k=1}^{\infty}\frac{1}{k}\left((12 + 3e^2)C_k^{0,1} + 6eC_k^{0,2} + e^2 C_k^{0,3}\right)\sin kM, \tag{78a}$$

$$\widehat{\widetilde{II}}_{12} = \widetilde{II}_{12} - \widetilde{\overline{II}}_{12} - \overline{II}_{12}(M - \pi)$$

$$= -\frac{1}{12}\sum_{k=1}^{\infty}\frac{1}{k}\left(3eC_k^{0,1} + 3C_k^{0,2} + eC_k^{0,3}\right)\sin kM, \tag{78b}$$

$$\widehat{\widetilde{III}}_{112} = \widetilde{III}_{112} - \widetilde{\overline{III}}_{112} - \overline{III}_{112}(M - \pi)$$

$$= -\frac{1}{96}\sum_{k=1}^{\infty}\frac{1}{k}\left(24C_k^{0,1} + 12eC_k^{0,2} + 8C_k^{0,3} + 3eC_k^{0,4}\right)\sin kM, \tag{78c}$$

$$\widehat{\widetilde{IV}}_{112} = \widetilde{IV}_{112} - \overline{\widetilde{IV}}_{112} - \overline{IV}_{112}(M - \pi)$$

$$= -\frac{1}{240} \sum_{k=1}^{\infty} \frac{1}{k} \left(30(2 + e^2)C_k^{0,1} + 60eC_k^{0,2} + 5(4 + 3e^2)C_k^{0,3} + 15eC_k^{0,4} + 3e^2 C_k^{0,5} \right) \sin kM, \quad (78d)$$

$$\widehat{\widetilde{IV}}_{222} = \widetilde{IV}_{222} - \overline{\widetilde{IV}}_{222} - \overline{IV}_{222}(M - \pi)$$

$$= -\frac{1}{240} \sum_{k=1}^{\infty} \frac{1}{k} \left(30(6 + e^2)C_k^{0,1} + 60eC_k^{0,2} - 5(4 - e^2)C_k^{0,3} - 15eC_k^{0,4} - 3e^2 C_k^{0,5} \right) \sin kM, \quad (78e)$$

and

$$\widetilde{\mathcal{II}} = \widetilde{II}_{11} - \overline{\widetilde{II}}_{11} - \widetilde{II}_{22} + \overline{\widetilde{II}}_{22}$$

$$= -\frac{1}{6} \sum_{k=1}^{\infty} \frac{1}{k} \left(3eS_k^{0,1} + 3S_k^{0,2} + eS_k^{0,3} \right) \cos kM, \quad (78f)$$

$$\widetilde{\mathcal{IV}} = \widetilde{I}_1 - \overline{\widetilde{I}}_1 + \widetilde{III}_{111} - \overline{\widetilde{III}}_{111} - \widetilde{III}_{122} + \overline{\widetilde{III}}_{122} - 5(\widetilde{IV}_{122} - \overline{\widetilde{IV}}_{122})$$

$$= -\frac{1}{48} \left[\sum_{k=1}^{\infty} \frac{1}{k} \left(6(2 + e^2)S_k^{0,1} + 36eS_k^{0,2} + (28 + 9e^2)S_k^{0,3} + 18eS_k^{0,4} + 3e^2 S_k^{0,5} \right) \cos kM \right]. \quad (78g)$$

C Numerical comparisons between Brouwer-Lyddane and Gim-Alfriend

Figures 10 through 13 show comparisons between the Brouwer-Lyddane and Gim-Alfriend formulations, as concerns the error maps of §4.
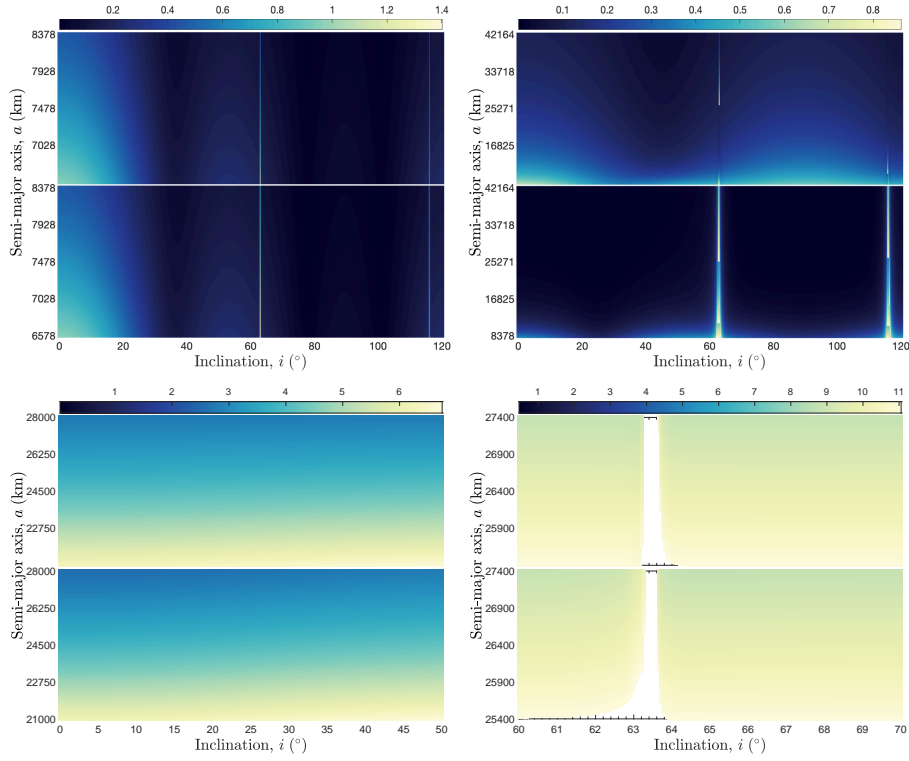
Fig. 10 Error maps in the inclination–semi-major axis plane using the Brouwer-Lyddane (*top* panels) and Gim-Alfriend (*bottom* panels) transformations, respectively. Each panel samples an equidistant grid of initial osculating (i, a) values, for initial eccentricities of 0.01 (*top-left*), 0.2 (*top-right*), 0.69 (*bottom-left*), and 0.74 (*bottom-right*), and where the initial mean anomaly, perigee, and node angles were all set to zero. The colorbar represents the norm RMS of the difference between the recovered and simulated positions over five orbital periods, according to each formulation. The colorbar limit was set to the maximum error found between the Milankovitch and numerical schemes (cf. Figs. 5 and 6), as the Brouwer-Lyddane formulation becomes singular near the critical inclination. Grid points leading to unphysical errors or to values that exceed this limit are represented in *white*. Clockwise starting from the *top left*: Brouwer-Lyddane recorded *(maximum, mean)* errors (in km) of $(1.0626, 0.1967)$, $(68.9371, 0.1804)$, $(6.7332, 4.3022)$, and $(1689.0290, 19.5805)$; and Gim-Alfriend recorded errors of $(1.3476, 0.1967)$, $(65.1025, 0.0728)$, $(3.4344, 0.0914)$, and $(1470.5632, 18.7458)$.
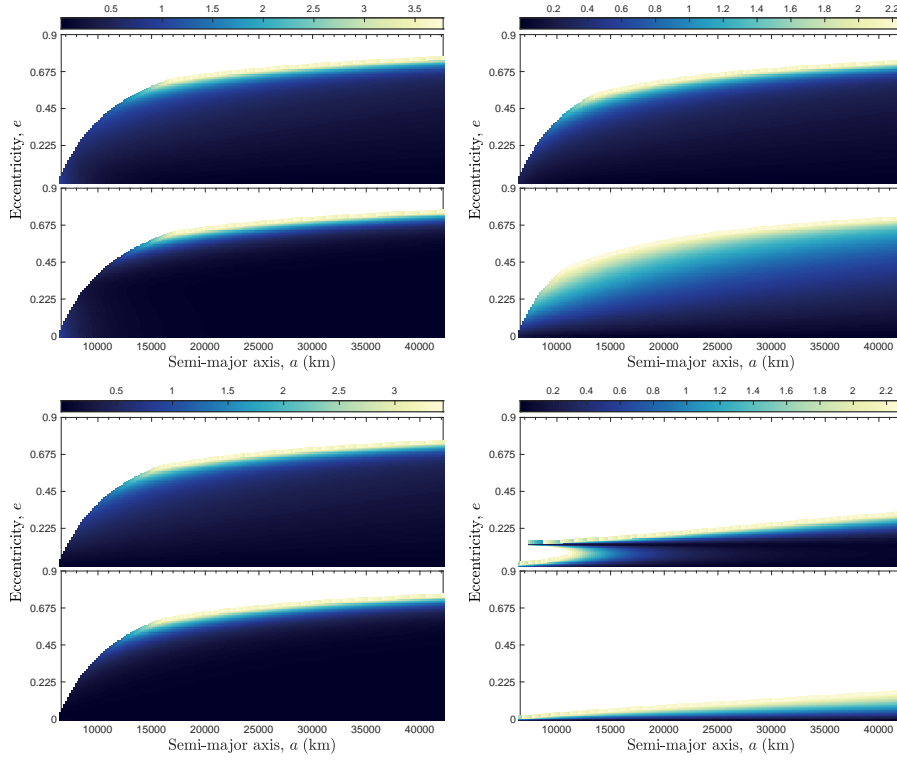
28

Fig. 11 Error maps in the semi-major axis–eccentricity plane using the Brouwer-Lyddane (*top* panels) and Gim-Alfriend (*bottom* panels) transformations, respectively. Each panel samples an equidistant grid of initial osculating (a, e) values, for initial inclinations of $6°$ (*top-left*), $63°$ (*top-right*), $98°$ (*bottom-left*), and $116.6°$ (*bottom-right*), and where the initial mean anomaly, perigee, and node angles were all set to zero. The colorbar represents the norm RMS of the difference between the recovered and simulated positions over five orbital periods, according to each formulation. The colorbar limit of each map was set to the maximum error found in the Milankovitch scheme (cf. Fig. 7) to provide a better contrast. Grid points leading to unphysical errors or to values that exceed this limit are represented in *white*. Clockwise starting from the *top left*: Brouwer-Lyddane recorded *(maximum, mean)* errors (in km) of $(58.5237, 1.2662)$, $(59.5538, 1.2013)$, $(59.6549, 1.2698)$, and $(82198.6187, 218.0410)$; and Gim-Alfriend recorded errors of $(58.4994, 1.0281)$, $(59.8837, 1.6868)$, $(59.6433, 1.0878)$, and $(48982.3446, 196.3659)$.
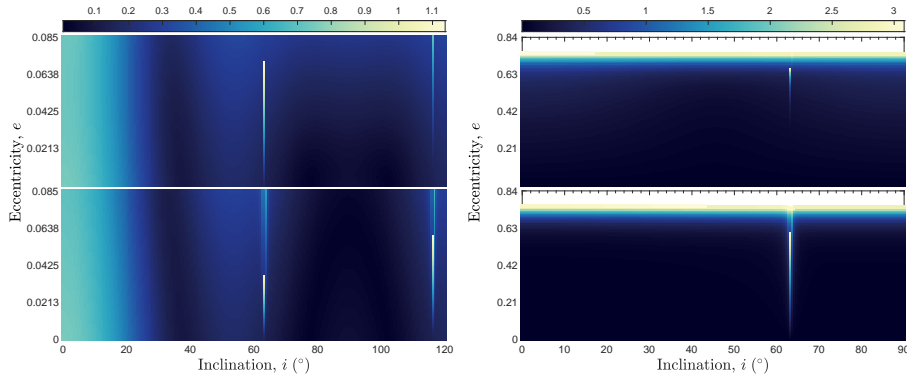

Fig. 12 Error maps in the inclination–eccentricity plane using the Brouwer-Lyddane (*top*) and Gim-Alfriend (*bottom*) transformations, respectively. Each panel samples an equidistant grid of initial osculating (i, a) values, for initial semi-major axes of $R + 800$ km (*left*) and a_{GEO} (*right*), and where the initial mean anomaly, perigee, and node angles were all set to zero. The colorbar represents the norm RMS of the difference between the recovered and simulated positions over five orbital periods, according to each formulation. The colorbar limit of each map was set to the maximum error found in the Milankovitch scheme (cf. Fig. 8) to provide a better contrast. Grid points leading to unphysical errors or to values that exceed this limit are represented in *white*. From *left* to *right*, the *(maximum, mean)* errors (in km) were $(1.2992, 0.2601)$ and $(94.1968, 1.9108)$ for Brouwer-Lyddane, and $(2.5030, 0.2355)$ and $(80.6873, 1.8132)$ for Gim-Alfriend.
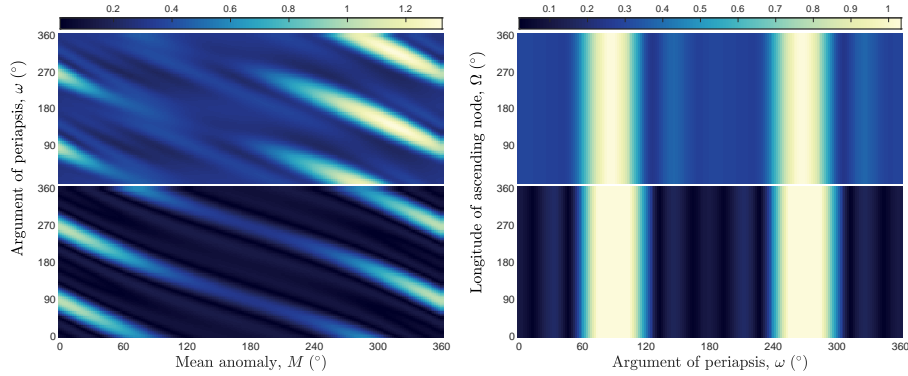
Fig. 13 Error maps in the mean anomaly–periapsis angle plane (*left*) and periapsis–node angles plane (*right*) using the Brouwer-Lyddane (*top*) and Gim-Alfriend (*bottom*) transformations, respectively. Each panel samples an equidistant grid of initial osculating (M, ω) or (ω, Ω) values, for an initial semi-major axis of $R + 800$ km, eccentricity of 0.1, and inclination of 98°. The remaining orbital element needed to form the full state vector was set to zero in each case. The colorbar represents the norm RMS of the difference between the recovered and simulated positions over five orbital periods, according to each formulation. The colorbar limit was set to the maximum error found across all schemes (cf. Fig. 9, as there were no singular or outlier cases for these maps). From *left* to *right*, the *(maximum, mean)* errors (in km) were $(1.3241, 0.4100)$ and $(1.0332, 0.4704)$ for Brouwer-Lyddane, and $(1.0173, 0.2060)$ and $(1.3206, 0.4133)$ for Gim-Alfriend.

References

Aksnes K (1972) On the use of the Hill variables in artificial satellite theory: Brouwer's theory. Astronomy and Astrophysics 17:70–75

Alfriend KT, Vadali SR, Gurfil P, How JP, Breger LS (2009) Spacecraft Formation Flying: Dynamics, Control and Navigation. Butterworth-Heinemann, Oxford

Battin RH (1999) An Introduction to the Mathematics and Methods of Astrodynamics, revised edn. AIAA, Reston

Breakwell JV, Vagners J (1970) On error bounds and initialization in satellite orbit theories. Celestial Mechanics 2:253–264

Brouwer D (1959) Solution of the problem of artificial satellite theory without drag. The Astronomical Journal 64:378–397

Brumberg V (1995) Analytical Techniques of Celestial Mechanics. Springer-Verlag, Berlin

Challe A, Laclaverie JJ (1969) Disturbing function and analytical solution of the problem of the motion of a satellite. Astronomy and Astrophysics 3:15–28

Coffey SL, Deprit A, Miller BR (1986) The critical inclination in artificial satellite theory. Celestial Mechanics 39:365–406

Deprit A (1969) Canonical transformations depending on a small parameter. Celestial Mechanics 1:12–30

Deprit A, Rom A (1970) The main problem of artificial satellite theory for small and moderate eccentricities. Celestial Mechanics 2:166–206

Ely TA (2015) Transforming mean and osculating elements using numerical methods. The Journal of the Astronautical Sciences 62:21–43

Garfinkel B (1959) The orbit of a satellite of an oblate planet. The Astronomical Journal 64:353–367

Giacaglia GEO (1976) A note on Hansen's coefficients in satellite theory. Celestial Mechanics 14:515–523

Gim DW, Alfriend KT (2003) State transition matrix of relative motion for the perturbed noncircular reference orbit. Journal of Guidance, Control, and Dynamics 26:956–971

Gurfil P, Lara M (2013) Motion near frozen orbits as a means for mitigating satellite relative drift. Celestial Mechanics and Dynamical Astronomy 116:213–227

Hoots FR (1981) Reformulation of the Brouwer geopotential theory for improved computational efficiency. Celestial Mechanics 24:367–375

Hoots FR, Glover RA, Schumacher Jr PW (2004) History of analytical orbit modeling in the U. S. Space Surveillance System. Journal of Guidance Control and Dynamics 27:174–185

Hori G (1966) Theory of general perturbations with unspecified canonical variables. Publications of the Astronomical Society of Japan 18:287–296

Hughes S (1981) The computation of tables of Hansen coefficients. Celestial Mechanics 29:101–107

Izsak IG (1963) A note on perturbation theory. The Astronomical Journal 68:559–561

Kaufman B (1981) First order semianalytic satellite theory with recovery of the short period terms due to third body and zonal perturbations. Acta Astronautica 8:611–623

Kozai Y (1959) The motion of a close Earth satellite. The Astronomical Journal 64:367–377

Kozai Y (1962a) Mean values of cosine functions in elliptic motion. The Astronomical Journal 67:311–312

Kozai Y (1962b) Second-order solution of artificial satellite theory without air drag. The Astronomical Journal 67:446–461

Lara M (2015a) Efficient formulation of the periodic corrections in Brouwer's gravity solution. Mathematical Problems in Engineering 2015:980,652

Lara M (2015b) LEO intermediary propagation as a feasible alternative to Brouwer's gravity solution. Advances in Space Research 56:367–376

Lara M (2018) Exploring sensitivity of orbital dynamics with respect to model truncation: The frozen orbits approach. In: Vasile M, Minisci E, Summerer L, McGinty P (eds) Stardust Final Conference. Astrophysics and Space Science Proceedings, Springer, Cham, pp 69–83

Lara M (2019) A new radial, natural, higher-order intermediary of the main problem four decades after the elimination of the parallax. Celestial Mechanics and Dynamical Astronomy 131, DOI 10.1007/s10569-019-9921-5

Le Fèvre C, Fraysse H, Morand V, Lamy A, Cazaux C, Mercier P, Dental C, Deleflie F, Handschuh DA (2014) Compliance of disposal orbits with the French Space Operations Act: The Good Practices and the STELA tool. Acta Astronautica 94:234–245

Levit C, Marshall W (2011) Improved orbit prediction using two-line elements. Advances in Space Research 47:1107–1115

Lyddane RH (1963) Small eccentricities or inclinations in the Brouwer theory of the artificial satellite. The Astronomical Journal 68:555–558

Nie T, Gurfil P, Zhang S (2019) Semi-analytical model for third-body perturbations including the inclination and eccentricity of the perturbing body. Celestial Mechanics and Dynamical Astronomy 131, DOI 10.1007/s10569-019-9905-5

Proulx RJ, McClain WD (1988) Series representations and rational approximations for Hansen coefficients. Journal of Guidance, Control, and Dynamics 11:313–319

Rosengren AJ, Scheeres DJ (2013) Long-term dynamics of high area-to-mass ratio objects in high-Earth orbit. Advances in Space Research 52:1545–1560

Rosengren AJ, Scheeres DJ (2014) On the Milankovitch orbital elements for perturbed Keplerian motion. Celestial Mechanics and Dynamical Astronomy 118:197–220

Roy AE, Moran PE (1973) Studies in the application of recurrence relations to special perturbation methods III. Non-singular differential equations for special perturbations. Celestial Mechanics 7:236–255

Sanders JA, Verhulst F, Murdock J (2007) Averaging Methods in Nonlinear Dynamical Systems, 2nd edn. Springer, New York

Schaub H, Alfriend TK (2001) J_2 invariant relative orbits for spacecraft formations. Celestial Mechanics and Dynamical Astronomy 79:75–95

Schaub H, Junkins JL (2018) Analytical Mechanics of Space Systems, 4th edn. American Institute of Aeronautics and Astronautics, Reston

Scheeres DJ (2012) Orbital Motion in Strongly Perturbed Environments: Applications to Asteroid, Comet and Planetary Satellite Orbiters. Springer-Praxis, Berlin

Shen HX, Kuai ZZ, Li HN (2019) Propagation and transformation of mean elements at geostationary orbits. Journal of Guidance, Control, and Dynamics 42:2132–2142

Uphoff C (1973) Numerical averaging in orbit prediction. AIAA Journal 11:1512–1516

Walter HG (1967) Conversion of osculating orbital elements into mean elements. The Astronomical Journal 72:994–997

Ward GN (1962) On the secular variations of the elements of satellite orbits. Proceedings of the Royal Society of London A 266:130–142